

Syracuse University

**SURFACE**

---

Dissertations - ALL

SURFACE

---

December 2019

## Strongly coupled fermions on the lattice

Nouman Tariq Butt  
*Syracuse University*

Follow this and additional works at: <https://surface.syr.edu/etd>



Part of the [Physical Sciences and Mathematics Commons](#)

---

### Recommended Citation

Butt, Nouman Tariq, "Strongly coupled fermions on the lattice" (2019). *Dissertations - ALL*. 1113.  
<https://surface.syr.edu/etd/1113>

This Dissertation is brought to you for free and open access by the SURFACE at SURFACE. It has been accepted for inclusion in Dissertations - ALL by an authorized administrator of SURFACE. For more information, please contact [surface@syr.edu](mailto:surface@syr.edu).

# Abstract

Since its inception with the pioneering work of Ken Wilson, lattice field theory has come a long way. Lattice formulations have enabled us to probe the non-perturbative structure of theories such as QCD and have also helped in exploring the phase structure and classification of phase transitions in a variety of other strongly coupled theories of interest to both high energy and condensed matter theorists. The lattice approach to QCD has led to an understanding of quark confinement, chiral symmetry breaking and hadronic physics. Correlation functions of hadronic operators and scattering matrix of hadronic states can be calculated in terms of fundamental quark and gluon degrees of freedom. Since lattice QCD is the only well-understood method for studying the low-energy regime of QCD, it can provide a solid foundation for the understanding of nucleonic structure and interaction directly from QCD. Despite these successes problems remain.

In particular, the study of chiral gauge theories on the lattice is an outstanding problem of great importance owing to its theoretical implications and for its relevance to the electroweak sector of the Standard Model. However the construction of these theories is plagued by the emergence of massless chiral modes in the lattice theory which have no counterpart in the continuum theory. This is a topological obstruction known as the Nielsen-Ninomiya theorem and can be proven to hold under assumptions of translation invariance, chiral invariance and hermiticity of the lattice Hamiltonian. One strategy that was advocated by Eichten and Preskill (EP) early on in the field was to generate large masses for these additional chiral states by coupling them to additional composite fermions. These composite fermions would arise as bound states via an auxiliary Yukawa interaction. Hence in the continuum limit mirror modes will be forced to

decouple from the spectrum without breaking chiral symmetry.

This proposal led to many numerical studies of different models. Goltermann et.al critiqued this proposal by showing that in specific realizations of the EP model the required phase containing a four fermion condensate was separated from the massless phase needed for a chiral theory by an intermediate phase in which the gauge symmetry was spontaneously broken. This was proven in the large  $N$  limit where the model contains  $N$  flavors of fermion. It led to the idea that the four-fermion phase was a lattice artifact and further work on these models stopped. However in recent few years this picture has changed. In three dimensions several studies of an  $SU(4)$  invariant four-fermion model have provided evidence in favor of a direct transition between massless(PMW) phase and four-fermion(PMS) phase. The generation of a mass without breaking symmetries via a symmetric four fermion condensate has received a lot of interest within the condensed matter community. Indeed this mechanism has been employed to gap out edge modes of topological insulators without breaking any symmetries. Of course the question for high energy physics is whether these new four fermion models exhibit this same structure in four dimensions and, if so, can it be used in the context of the original EP proposal to create a lattice theory whose low energy excitations are chiral. In this thesis I discuss the progress towards this goal.

# Strong coupled fermions on the lattice

by

Nouman Tariq Butt

BS (Physics), Lahore University of Management Sciences, 2012

DISSERTATION

Submitted in partial fulfillment of the requirements for the degree of  
Doctor of Philosophy in Physics

Syracuse University

December 2019

Copyright 2019 Nouman Tariq Butt

All rights reserved

*To Abu, Anam, and Arya*

*In loving memory of Ismat Bano*

# Acknowledgements

First and foremost, I would like to thank my advisor, *Simon Catterall*, for his guidance and support throughout my graduate studies. His intuitive approach has helped me develop a deeper comprehension of diverse fields in physics. He had been very patient with my rather sluggish pace as Phd student and always afforded me time to develop understanding of subject under discussion. Without his faith and encouragement I couldn't have reached so far.

I wish to thank *Cristian Armendariz-Picon* and *Jay Hubisz* for being great instructors for difficult graduate-level courses. I was fortunate to have *Jay Hubisz* and *Jiji Fan* mentor me during my initial years. I would thank *Scott Watson* for his encouragement whenever I asked him for advice. I owe special thanks to *Carl Rosenzweig* for all the non-physics discussions we had all these years. I never got a chance to work with *Jack Laiho* but I have always stayed in awe of his work on dynamical triangulations. I would like to thank him for being there every time I needed his help.

When I started working with *Simon* I had the opportunity to learn from *David Schaich* for which I would like to thank him. Recently it had been a pleasure to benefit from *Judah Unmuth Yockey's* expertise in tensor networks. I wish to thank him for all our discussion on tensor networks. I am extremely grateful to *A.P.Balachandran* for answering my trivial questions on various aspects of QFTs in general and showing me his deeper insight into non-trivial problems.

I would thank all my friends - *Raghav Jha*, *Sourav Bhabesh*, *Prashant Mishra*, *Swetha Bhagwat*, *Gizem Sengor*, *Ogan Ozsay*, *Suraj Shankar*, *Francesco Serafin*, *Mohd. Asaduzzaman* for all the time we spent together and for all the insightful discussions we had. I would also express my gratitude to staff members *Patty Whitmore* and *Yudaisy Salomon Sargenton* who were always there to help with complex paper-work and administrative matters.

A special and heartfelt thanks to Anam for her unfaltering support all these years

and for bearing with me whenever I was in mentally aloof state. Finally I would thank my father for always supporting my choices, be it pursuing a career in natural science or any other familial affairs.



# List of Papers

Chapters 3, 4, 5 and 6 of the dissertation are comprised of the work carried out in the following papers, respectively:

1.  $SO(4)$  invariant Higgs-Yukawa model with reduced staggered fermions, [Phys. Rev. D \*\*98\*\*, 114514](#)
2. Topology and strong four fermion interactions in four dimensions, [Phys. Rev. D \*\*97\*\*, 094502](#)
3. Simulations of  $SU(2)$  lattice gauge theory with dynamical reduced staggered fermions, [Phys. Rev. D \*\*99\*\*, 014505](#)
4. Four fermion condensates in  $SU(2)$  Yang-Mills-Higgs theory on a lattice, [arXiv:1811.01015](#)

The following research work have not been included in the thesis due to their disjoint research field, irrelevance to the main theme of the dissertation work and because of their pre-print status

1. Tensor network study of massless Schwinger Model....*In progress*
2. Tensor network computation using Quantum Circuits...*Work done at ANL*

# Contents

<b>1</b>	<b>Lattice Fermions</b>	<b>1</b>
1.1	Introduction . . . . .	1
1.2	Naive fermions . . . . .	2
1.3	Staggered Fermions . . . . .	4
1.4	Reduced Staggered Fermions . . . . .	9
<b>2</b>	<b>Dynamical mass generation from four-fermion interactions</b>	<b>12</b>
2.1	Fermion mass without symmetry breaking . . . . .	12
2.2	Lattice model and symmetries . . . . .	13
2.3	Strong coupling expansion . . . . .	14
2.4	Auxiliary field representation . . . . .	16
2.5	Analytic arguments for phase structure . . . . .	18
<b>3</b>	<b><math>SO(4)</math> invariant Higgs-Yukawa model on lattice</b>	<b>20</b>
3.1	Introduction . . . . .	20
3.2	Action and Symmetries . . . . .	22
3.3	Analytical results . . . . .	23
3.4	Phase Structure . . . . .	26
3.5	Fermion Bilinears . . . . .	31
3.6	Resulting phase diagram . . . . .	36
3.7	Summary and Conclusions . . . . .	37

3.8	Appendix A . . . . .	39
3.9	Appendix B . . . . .	42
<b>4</b>	<b>Topology defects from four-fermion interactions</b>	<b>45</b>
4.1	Introduction . . . . .	45
4.2	Four fermion theory . . . . .	46
4.3	Aside: connection to (reduced) staggered fermions . . . . .	48
4.4	Auxiliary field action . . . . .	49
4.5	Effective Action . . . . .	50
4.6	Topological defects . . . . .	53
4.7	BKT transition . . . . .	56
4.8	Summary . . . . .	57
4.9	Appendix . . . . .	59
<b>5</b>	<b><math>SU(2)</math> lattice gauge theory with reduced staggered fermions</b>	<b>64</b>
5.1	Introduction . . . . .	64
5.2	Action and symmetries . . . . .	68
5.3	Numerical Results . . . . .	71
5.4	Summary . . . . .	78
<b>6</b>	<b>Four-fermion condensates in <math>SU(2)</math> Yang-Mills-Higgs theory on lattice</b>	<b>79</b>
6.1	Introduction . . . . .	79
6.2	Fermion kinetic term . . . . .	80
6.3	Imposing the reality condition . . . . .	81
6.4	Adding Yukawa interactions . . . . .	83
6.5	Reduction to $SO(4)$ model . . . . .	84
6.6	Numerical Results . . . . .	85
6.7	Summary . . . . .	87



# List of Figures

3.1	$\langle \sigma_+^2 \rangle$ vs $G$ for $L = 8$ , comparing $\kappa = \pm 0.05$ and $0$ . . . . .	27
3.2	$\chi_{\text{stag}}$ vs $G$ at $\kappa = 0$ for $L = 4, 8$ and $12$ . . . . .	28
3.3	$\chi_{\text{stag}}$ vs $G$ at $\kappa = -0.05$ for $L = 6, 8$ and $12$ . . . . .	29
3.4	$\chi_{\text{stag}}$ vs $G$ at $\kappa = 0.05$ for $L = 6, 8$ and $12$ . . . . .	29
3.5	The ferromagnetic susceptibility $\chi_f$ vs $G$ at $\kappa = 0.05$ for $L = 6, 8$ and $12$ . Unlike the other susceptibility plots, the y-axis scale is not logarithmic. . . . .	30
3.6	Average number of CG iterations for Dirac operator inversions on $L = 8$ lattices, plotted vs $G$ for $\kappa = 0$ and $0.05$ . . . . .	31
3.7	Four fermion condensate at $G = 2$ vs $\kappa$ for $L = 8$ . . . . .	32
3.8	Ferromagnetic and staggered magnetizations at $G = 2$ vs $\kappa$ for $L = 8$ . . . . .	32
3.9	Antiferromagnetic bilinear condensate vs $m_2$ (with $m_1 = 0$ ) at $(\kappa, G) =$ $(0, 1.05)$ for $L = 8, 12$ and $16$ . . . . .	33
3.10	Antiferromagnetic bilinear condensate vs $m_2 = m_1$ at $(\kappa, G) = (-0.05, 1.05)$ for $L = 6, 8$ and $12$ . . . . .	34
3.11	Antiferromagnetic (left) and ferromagnetic (right) bilinear condensates vs $m_2 = m_1$ at $(\kappa, G) = (0.05, 1.05)$ for $L = 6, 8$ and $12$ . . . . .	35
3.12	Sketch of the phase diagram in the $(\kappa, G)$ plane. . . . .	36
3.13	Antiferromagnetic (left) and ferromagnetic (right) bilinear condensates vs $m_2 = m_1$ at $(\kappa, G) = (0.085, 1.05)$ for $L = 6, 8$ and $12$ . . . . .	40

3.14	Ferromagnetic bilinear condensate vs $m_2 = m_1$ at $(\kappa, G) = (0.1, 1.1)$ for $L = 6, 8$ and $12$ . . . . .	41
3.15	The $L = 8$ ferromagnetic susceptibility $\chi_f$ vs $G$ for $\kappa = 0, 0.05$ and $0.1$ . . . . .	41
3.16	Four fermion condensate on vs $G$ for $L = 8$ , comparing $\kappa = 0.5$ and $0.1$ . . . . .	42
5.1	$\langle O_S \rangle$ with $m = m_1 = 0.1$ for $L = 6, 8, 12$ . . . . .	72
5.2	$\langle O_L \rangle$ with $m = m_1 = 0.1$ for $L = 6, 8, 12$ . . . . .	72
5.3	$\langle  L_p(x)  \rangle$ Polyakov line for $L = 6$ and $m = 0.1$ . . . . .	73
5.4	$\langle O_S \rangle$ vs $m$ at $\beta = 1.8$ for $L = 6, 8, 12, 16$ . . . . .	74
5.5	$\langle O_L \rangle$ vs $m_1$ at $\beta = 1.8$ for $L = 6, 8, 12, 16$ . . . . .	74
5.6	$\langle O_S \rangle$ vs $m$ at $\beta = 1.7$ for $L = 6, 8, 12, 16$ . . . . .	76
5.7	$\langle O_L \rangle$ vs $m_1$ at $\beta = 1.7$ for $L = 6, 8, 12, 16$ . . . . .	76
5.8	$\langle C(t) \rangle$ : pion correlator with quark mass $m = 0.2$ for $8^3 \times 32$ . . . . .	77
5.9	$m_\pi$ vs $m$ : Pion mass vs bare quark mass for $8^3 \times 32$ . . . . .	77
6.1	Four-fermion condensate(left) and $Tr(\phi^2)$ (right) vs $G$ with $\beta = \infty$ for $L = 4$ . . . . .	86
6.2	Four-fermion condensate(left) and $Tr(\phi^2)$ (right) vs $1/\beta$ with $G = 0.5$ for $L = 4$ . . . . .	86

# List of conventions and symbols

Throughout this dissertation, we have adopted the following conventions:

- Greek indices  $\mu, \nu, \lambda, \dots$  label the components of lattice vectors with respect to the coordinate basis and take values 0, 1, 2, 3.
- Latin indices  $a, b, c, \dots$  run over the spatial coordinates and take the values 1, 2, 3.
- Repeated indices are summed over.
- We work in units such that  $\hbar = c = 1$ . This results in units where  $[\text{Mass}] = [\text{Energy}] = [\text{Momentum}] = [\text{Length}^{-1}] = [\text{Time}^{-1}]$ .

Throughout this dissertation, we have used the following abbreviations:

- EFT: Effective Field Theory
- QED: Quantum Electrodynamics
- QCD: Quantum Chromodynamics
- QFT: Quantum field theory
- SM: Standard Model
- PMS: Paramagnetic Strong
- PMW: Paramagnetic Weak
- AFM: Anti-Ferromagnetic
- FM: Ferromagnetic
- vev: vacuum expectation value
- EP: Eitichen-Preskill

# Chapter 1

## Lattice Fermions

### 1.1 Introduction

The standard model of particle physics has successfully explained to great extent the plethora of particles discovered so far. Basic constituents of the SM include families of leptons and quarks with diverse gauge couplings to various force-carriers. In particular, quark confinement in QCD leads to break down of conventional perturbation theory and makes non-perturbative dynamics of SM fermions inaccessible. The application of lattice methods to fermion theories with gauge fields has increased our understanding of non-perturbative sector by making use of numerical simulations. However putting fermions on the lattice gives rise to fermion doubling which transforms a continuum chiral theory into vector-like on the lattice. Moreover in lattice formalism we need to have a well-defined continuum limit which is imperative for the validity of physics extracted from lattice dynamics. In this context it is important to overcome this obstacle to ensure existence of continuum chiral gauge theories and to study their non-perturbative dynamics using lattice methods. This requires construction of lattice fermions in a framework devoid of any doubling and with the right



continuum limit. In the next few sections we review lattice fermions, species doubling and proposed solutions. We emphasize more on staggered fermions since we are going to use staggered construction and it's *reduced* formalism for the rest of this dissertation. Briefly, we also discuss gauge fields on the lattice.

## 1.2 Naive fermions

In this section we review the discretization of the fermion action. Starting with the euclidean Dirac action given by

$$S_F = \int d^4x \bar{\psi}(\gamma_\mu \partial_\mu + m)\psi(x) \quad (1.1)$$

we discretize the action by introducing a lattice where continuous positions are replaced by discrete points and integrals by discrete sums over the lattice. The discretized action takes the following form

$$S_F^{lattice} = \sum_x a^4 \left( \frac{1}{2a} \sum_\mu \bar{\psi}(x) \gamma_\mu \delta_\mu \psi(x) + \bar{\psi}(x) \psi(x) \right) \quad (1.2)$$

where  $\delta_\mu$  is symmetric difference operator with the action

$$\delta_\mu \psi(x) = \frac{1}{2a} [\psi(x + \mu) - \psi(x - \mu)] \quad (1.3)$$

and  $\gamma_\mu$  are euclidean gamma matrices satisfying a Clifford algebra. Transforming to momentum space the naive fermion propagator obtained is

$$\langle \psi_\alpha \bar{\psi}_\beta \rangle = \int_{-\frac{\pi}{a}}^{\frac{\pi}{a}} \frac{d^4p}{(2\pi)^4} \frac{[-i \sum_\mu \gamma_\mu \tilde{p}_\mu + m]_{\alpha\beta}}{\sum_\mu \tilde{p}_\mu^2 + M^2} \quad (1.4)$$

where  $\alpha, \beta$  are spinor indices and  $\tilde{p}_\mu$  is defined as

$$\tilde{p}_\mu = \frac{1}{a} \sin(p_\mu a) \quad (1.5)$$

In the limit  $a \rightarrow 0$  this propagator will reduce to the continuum Dirac propagator but with sixteen poles rather than a single one. The emergence of these extra poles of the fermion propagator is called species doubling or more commonly known as fermion doubling. These poles can be interpreted as additional flavors in the continuum limit. In real space this doubling is associated with a set of fifteen invariances of the lattice action given by

$$\begin{aligned} \psi(x) &\rightarrow (-1)^{x_\mu} \gamma_\mu \gamma_5 \psi(x), & \psi(x) &\rightarrow (-1)^{x_\mu} (-1)^{x_\nu} \gamma_\mu \gamma_5 \gamma_\nu \gamma_5 \psi(x) \\ \psi(x) &\rightarrow i\varepsilon(x) (-1)^{x_\mu} \gamma_\mu \psi(x), & \psi(x) &\rightarrow i\varepsilon(x) \gamma_5 \psi(x) \end{aligned} \quad (1.6)$$

These 15 symmetry generators generate an  $SU(4)$  flavor symmetry. In general the doubling symmetry relates sixteen corners of Brillouin zone, up to a reshuffling of spinor indices. Since the propagator is invariant under these transformations there are sixteen energetically degenerate species (modes) having the same mass  $m$  in the continuum limit. Each of these modes contribute to the axial anomaly in a specific pattern leading to a vanishing of the anomaly in the lattice theory. In general in  $d$  space-time dimensions we will have  $2^d$  additional species (modes) for each fermion. Wilson proposed a solution for this problem with the addition of a second-order derivative term which only couples to the doubler modes with momentum dependent masses for each doubler mode. In the continuum limit all the doubler modes become infinitely massive, thus decoupling from the spectrum, leaving behind a single primary fermion. However the Wilson term explicitly breaks chiral symmetry as it becomes a Dirac type mass term in the continuum. We will discuss in chapter 3 how a generalized Wilson term can be used in our formulation to gap out doublers without explicitly

breaking chiral symmetry. Another resolution was proposed by Kogut-Susskind which goes by the name of staggered fermions in the lattice literature. Next we will describe the staggered fermion formulation.

### 1.3 Staggered Fermions

The naive fermions describe sixteen continuum fermions. The staggered fermion reduces this to four using a trick called *spin diagonalization* which can be achieved by the following transformations

$$\psi(x) \rightarrow U(x)\chi(x), \quad \bar{\psi}(x) \rightarrow \bar{\chi}(x)U^\dagger(x) \quad (1.7)$$

where  $U(x)$  are  $2^{\frac{d}{2}} \times 2^{\frac{d}{2}}$  unitary matrices with the property

$$U^\dagger(x)\gamma_\mu U(x+\mu) = \eta_\mu(x)I \quad (1.8)$$

The following unitary matrix  $U(x)$  satisfies the equation above

$$U(x) = \gamma_1^{x_1}\gamma_2^{x_2}\dots\gamma_d^{x_d} \quad (1.9)$$

with phases  $\eta_\mu(x)$  defined as

$$\eta_\mu(x) = (-1)^{\sum_{i=1}^{d-1} x_i} \quad (1.10)$$

Using single component staggered field  $\chi(x)$  we can write action (Eq. 1.1) as

$$S_F = \sum_{x,\mu,\alpha} \eta_\mu(x)\bar{\chi}_\alpha(x)\Delta_\mu\chi_\alpha(x) + m \sum_x \bar{\chi}_\alpha(x)\chi_\alpha(x) \quad (1.11)$$

There are no gamma matrices left in the action. The staggered action with

index  $\alpha = 1, 2, \dots$  has  $2^{\frac{d}{2}}$  redundant copies. Thus we can choose a single copy and write an action with no spinor indices as

$$S_F^{stag} = \sum_{x,\mu} \eta_\mu(x) \bar{\chi}(x) [\chi(x + \mu) - \chi(x - \mu)] + m \sum_x \bar{\chi}(x) \chi(x) \quad (1.12)$$

Now we have only one d.o.f per lattice site with the  $\eta_\mu(x)$  phases remnants of the Dirac gamma matrices. They satisfy an anti-commutation relation given by

$$\eta_\mu(x) \eta_\nu(x + \mu) + \eta_\nu(x) \eta_\mu(x + \nu) = 2\delta_{\mu\nu} \quad (1.13)$$

Using appropriate linear combination of staggered fields in the hypercube we can write single component staggered action as  $2^{\frac{d}{2}}$  flavored Dirac field  $\psi^a$  where  $a = 1, 2, \dots, 2^{\frac{d}{2}}$  with components given by  $\psi_\alpha^a$  where  $\alpha$  is spinor index. This restructured action can be used to take continuum limit which produces  $2^{\frac{d}{2}}$  flavors of Dirac fermions in the continuum.

We have thus reduced the number of doubler modes by a factor of four with spin diagonalization and transforming to single component staggered fields. Without removing redundant copies of staggered action from eqn 1.11 we would still have full  $SU(4)$  doubling symmetry with no space-time dependence. This projection to a single component staggered field makes all symmetries except color and flavor  $x$  dependent. The translation to naive fermions now takes the following form

$$\psi(x) \rightarrow \psi(x + \mu) \implies \Phi(x) \rightarrow \xi_\mu(x) \gamma_\mu \Phi(x + \mu) \quad (1.14)$$

where  $\Phi$  is four-component spinor and  $\xi_\mu(x) = (-1)^{\sum_{i=\mu+1}^d x_i}$ . We can't simply project it down to single component staggered field since the projection doesn't commute with lattice translational symmetry. However a combination of the doubling transformation with single link translations called *shifts* realize

a pseudo-translation on staggered fields.

$$\psi(x) \rightarrow i\varepsilon(x)(-1)^{x_\mu}\gamma_\mu\psi(x + \mu) \implies \chi(x) \rightarrow \xi_\mu(x)\chi(x + \mu) \quad (1.15)$$

A normal lattice translation can be realized using  $\xi_\mu(x)\xi_\mu(x + \mu) = 1$ . However this is translation by twice the lattice spacing.

With *shift* symmetry realized as pseudo-translation, other lattice symmetries satisfied by staggered fermions are

1. Space-time rotation

$$\chi(x) \rightarrow M_\Lambda(\Lambda^{-1}x)\chi(\Lambda^{-1}x) \quad (1.16)$$

where  $\Lambda^{\mu\nu}$  is a rotation on lattice co-ordinates and

$M_\Lambda = \frac{1}{2}(1 \pm \eta_\mu(x)\eta_\nu(x) \mp \xi_\mu(x)\xi_\nu(x) + \eta_\mu(x)\eta_\nu(x)\xi_\mu(x)\xi_\nu(x))$  is a pure phase with sign convention  $\pm$  if  $\mu > \nu$  and  $\mp$  if  $\mu < \nu$

2. Axis Reversal

$$\chi(x) \rightarrow (-1)^\mu\chi(I^\mu x) \quad (1.17)$$

where  $I^\mu(x)$  is axis reversal operation such that  $x_\mu \rightarrow -x_\mu$  and  $x_\nu \rightarrow x_\nu$  where  $\nu \neq \mu$ .

The symmetries above have a well-defined continuum limit for staggered fermions. For example the hypercubic rotation  $\Lambda_{\mu\nu} \rightarrow SO(4)$  in the continuum. However the doubling symmetry of naive fermions now takes the form of a discrete subgroup of  $SU(4)$  namely  $\Gamma_4$  generated by *shifts*  $S_\mu = \xi_\mu(x)$  satisfying anti-commutation relation

$$S_\mu S_\nu + S_\nu S_\mu = 2\delta_{\mu\nu} \quad (1.18)$$

$\Gamma_4$  is smallest subgroup contained in  $SU(4)$  doubling group with 32 elements. In momentum space  $S_\mu$  furnishes a 4-dimensional fermionic representation which is more commonly known as the taste-basis. Taste (flavor)  $SU(4)$  symmetry of naive fermions have been explicitly broken down to  $\Gamma_4$  by staggered fermions whilst the  $2^d$  doubler modes associated with naive fermions have been reduced to  $2^{\frac{d}{2}}$  modes. Staggered fermions have no Dirac structure of course so there is no notion of left and right-handed fields<sup>1</sup>. Axial symmetry after spin diagonalisation then takes the following form

$$\psi(x) \rightarrow \gamma_5 \psi(x) \implies \Phi(x) \rightarrow \gamma_5 \varepsilon(x) \Phi(x) \quad (1.19)$$

where  $\Phi$  is a spinor in spin-diagonal basis. From this transformation it's easy to see that this symmetry won't survive projection onto single component staggered fields. We can define a more generic transformation which maps  $\gamma_5$  to unity under staggering, but it won't be an axial transformation exactly. Another important feature of the transformation in (1.19) is the appearance of  $\varepsilon(x)$  which behaves like  $\gamma_5$  for staggered fields. An important symmetry of continuum Dirac operator as well as lattice fermion operator is  $\gamma_5$  – *hermiticity*

$$(\gamma_5 D)^\dagger = \gamma_5 D \iff \gamma_5 D \gamma_5 = D^\dagger \quad (1.20)$$

This  $\gamma_5$  – *hermiticity* takes a unique form in the staggered formalism with  $\gamma_5$  replaced by  $\varepsilon(x)$  satisfying

$$D(x, y)^\dagger = \varepsilon(x) D(x, y) \varepsilon(y) \quad (1.21)$$

where  $D(x, y)$  is the staggered fermion operator. This property implies anti-

---

<sup>1</sup>In analogy with left and right-handed fields we can define even(odd) projectors  $P_{e,o} = \frac{1 \pm \varepsilon(x)}{2}$  on fermion field components living on even and odd sites

hermiticity of the staggered operator

$$D^\dagger = -D \tag{1.22}$$

which arises from the following property

$$\varepsilon(x)\varepsilon(x + \mu) = -1 \tag{1.23}$$

From this we deduce that the staggered action has a residual chiral symmetry emerging from peculiar properties associated with  $\varepsilon(x)$ . In chiral limit we have  $U(1)_\varepsilon$  symmetry

$$\chi \rightarrow e^{i\alpha\varepsilon(x)}\chi \quad \bar{\chi}(x) \rightarrow \bar{\chi}(x)e^{i\alpha\varepsilon(x)} \tag{1.24}$$

which is an axial-like transformation however it is a taste non-singlet and is spontaneously broken with  $\varepsilon(x)\bar{\chi}(x)\chi(x)$  as interpolating field. It's obvious from (1.24) that fields on even and odd sites transform differently. Using this fact we can realize the flavor symmetry in the following way

$$\chi(x) \rightarrow e^{iT^a\theta^a\varepsilon(x)}\chi(x) \quad \bar{\chi}(x) \rightarrow \bar{\chi}(x)e^{iT^a\theta^a\varepsilon(x)} \tag{1.25}$$

where  $T^a$  are flavor generators of  $U(N)$ . Another way of representing this transformation by realizing independent transformations on even and odd sites is given by

$$\begin{aligned} \chi_e &\rightarrow U_e\chi_e, \bar{\chi}_o \rightarrow \bar{\chi}_o U_e^\dagger, U_e \in U_e(N) \\ \bar{\chi}_e &\rightarrow \bar{\chi}_e U_o^\dagger, \chi_o \rightarrow U_o\chi_o, U_o \in U_o(N) \end{aligned} \tag{1.26}$$

where  $\chi_e$  represents  $\chi(x)$  on even sites while  $\chi_o$  represents  $\chi(x)$  on odd sites. Staggered kinetic term is invariant under these transformations which form

$U_e(N_f) \otimes U_o(N_f)$  chiral-flavor symmetry<sup>2</sup>. Similarly we have a vector-flavor symmetry satisfied by kinetic term.

$$\chi(x) \rightarrow e^{iT^a \theta^a} \chi(x) \quad \bar{\chi}(x) \rightarrow \bar{\chi}(x) e^{-iT^a \theta^a} \quad (1.27)$$

Gauge fields can be introduced for the staggered fermion with a slight modification to *shift* symmetry transformation which now includes transformation for the gauge links as well. The staggered action with gauge fields reads

$$S_F^{stag} = \sum_{x,\mu} \eta_\mu(x) [\bar{\chi}(x) U_\mu(x) \chi(x+\mu) - \bar{\chi}(x) U_\mu^\dagger(x-\mu) \chi(x-\mu)] + m \sum_x \bar{\chi}(x) \chi(x) \quad (1.28)$$

and *shift* symmetry  $S_\mu$  is given by

$$\begin{aligned} \chi(x) &\rightarrow \xi_\mu(x) \chi(x+\mu) \\ \bar{\chi}(x) &\rightarrow \xi_\mu(x) \bar{\chi}(x+\mu) \\ U_\nu(x) &\rightarrow U_\nu(x+\mu) \quad \forall \nu \end{aligned} \quad (1.29)$$

## 1.4 Reduced Staggered Fermions

Staggered fermion reduces doubling from  $2^d$  species to  $2^{\frac{d}{2}}$  through spin diagonalisation. This can be further improved by using the *reduced* staggered formalism. We simply restrict the fields  $\chi$  to odd sites and  $\bar{\chi}(x)$  to even sites using even(odd) projectors.

$$\begin{aligned} \chi(x) &\rightarrow \frac{1 - \varepsilon(x)}{2} \chi(x) \\ \bar{\chi}(x) &\rightarrow \bar{\chi}(x) \frac{1 + \varepsilon(x)}{2} \end{aligned} \quad (1.30)$$

---

<sup>2</sup>For gauge group  $SU(3)$  this symmetry possess the right continuum limit however for  $SU(2)$  symmetry breaking pattern doesn't give the right continuum limit.



By restricting  $\bar{\chi}$  to even sites we can identify it as an independent field by dropping the bar and re-labeling it as  $\chi$ . This produces a "real" or Majorana-like staggered fermion with action given by

$$S = -\frac{1}{2} \sum_{x,\mu} \eta_\mu(x) \chi(x) \chi(x + \mu) \quad (1.31)$$

Here we emphasize that the *reduced* staggered action is invariant under the full-staggered symmetry group. It is easy to verify that [(1.15)-(1.17)] is satisfied along with global  $U(1)$  transformation of the form  $\chi(x) \rightarrow e^{i\alpha\varepsilon(x)}\chi(x)$ . An important consequence of this formalism is the non-existence of a single site mass term since  $\chi(x)\chi(x)$  vanishes due to Grassmann nature. However a disadvantage arises when you want to write an action with flavor symmetry. We can only use groups with real or pseudo-real representations as flavor groups for *reduced* staggered formalism. Gauge fields can be introduced in a straight-forward manner starting with the full staggered action in (1.28). Restricting fields  $\bar{\chi}(x)$  to even sites and  $\chi(x)$  to odd sites we get *reduced* gauged action

$$S = -\frac{1}{2} \sum_{x,\mu} \eta_\mu(x) \chi^T(x) \mathcal{U}_\mu(x) \chi(x + \mu) \quad (1.32)$$

where  $\mathcal{U}_\mu(x)$  is defined as:

$$\mathcal{U}_\mu(x) = \frac{1 + \varepsilon(x)}{2} U_\mu(x) + \frac{1 - \varepsilon(x)}{2} U_\mu^*(x) \quad (1.33)$$

The action in (1.32) has a global  $U(1)$  invariance and is also *shift* symmetric.

The  $U(1)$  invariance is

$$\chi(x) \rightarrow e^{i\alpha\varepsilon(x)}\chi(x) \quad (1.34)$$

and *shift* symmetry is given by

$$\chi(x) \rightarrow \pm \xi_\mu(x) \psi(x + \mu), \quad U_\nu(x) \rightarrow U_\nu^*(x + \mu) \quad (1.35)$$

Other symmetries in [(1.16)-(1.17)] also hold true in the gauged construction of *reduced* formalism. *Shift* symmetries can be interpreted as discrete remnant of continuum chiral symmetries [26]. A gauge invariant operator which breaks *shift* symmetry is given by

$$O = \sum_{x_\mu} \varepsilon(x) \xi_\mu(x) \chi(x) [\mathcal{U}_\mu(x) \chi(x + \mu) + \mathcal{U}_\mu^\dagger(x - \mu) \chi(x - \mu)] \quad (1.36)$$

This operator in the continuum will take form of a mass term which breaks chiral symmetry. We can set gauge links  $U_\mu(x) = \infty$  to get the non-gauged version of this operator. Many other link bilinear operators can be constructed in *reduced* staggered formalism using fields in hypercube but each of them have a different continuum interpretation. The spectrum of such possible operators have been discussed in detail in Ref. [4]. At this point we have developed enough machinery for full staggered and *reduced* staggered formalisms to explore more generic models with flavor(gauge) symmetries.

# Chapter 2

## Dynamical mass generation from four-fermion interactions

### 2.1 Fermion mass without symmetry breaking

We introduce four dimensional lattice model with four-fermion interactions invariant under an  $SO(4)$  symmetry. This model is motivated by work of [1, 2] who constructed  $SU(4)$  invariant theory in three dimensions and provided numerical evidence that system can dynamically *generate* mass for fermions without breaking any symmetry. Mechanism of symmetric mass generation is novel in the sense that there exist no local order parameter that differentiates between massless and massive phases of the system. We choose  $SO(4)$  over  $SU(4)$  because latter would cause a sign problem for rational hybrid Monte Carlo algorithm. We use *reduced* staggered formalism for constructing this model which ensures absence of single-site  $SO(4)$  invariant mass term. Infact without the mass term our model also satisfies  $SU(4)$  symmetry. In order to construct  $SO(4)$  invariant mass term we can use one-link mass term using fields in the hypercube.  $SO(4)$  and *shift* symmetries can spontaneously break through condensation of

bilinear and one-link mass terms induced via quantum corrections. We develop analytic arguments that for large four-fermi coupling only four-fermion condensate survives. Moreover using strong-coupling expansion we show that fermion propagator is massive at critical value of four-fermi coupling.

## 2.2 Lattice model and symmetries

Consider a theory four *reduced* staggered fermions in four dimensions with action containing on-site  $SU(4)$  invariant four-fermion interaction. Action is given by

$$S = \frac{1}{2} \sum_{x,\mu} \eta^\mu(x) \psi^a \Delta_\mu^{ab} \psi^b - \frac{G^2}{4} \sum_x \varepsilon_{abcd} \psi^a \psi^b \psi^c \psi^d \quad (2.1)$$

where  $\Delta_\mu^{ab} \psi^b = \delta^{ab}[\psi^b(x + \mu) - \psi^a(x - \mu)]$  and  $\eta_\mu(x)$  are staggered phases described in (1.10).  $\psi^a$  is in fundamental representation of  $SU(4)$  and transform as following

$$\psi \rightarrow e^{i\alpha\varepsilon(x)} \psi \quad (2.2)$$

with  $\alpha$  an element in  $SU(4)$  algebra. Kinetic part of action also satisfies global  $U(1)$  symmetry given by

$$\psi \rightarrow e^{i\theta\varepsilon(x)} \psi \quad (2.3)$$

however with addition of four-fermion interaction this symmetry is explicitly broken to  $Z_4$  whose action is given by  $\psi \rightarrow \Gamma\psi$  where  $\Gamma = [1, -1, i\varepsilon(x), -i\varepsilon(x)]$ . All other staggered symmetries involving *shifts*, axis reversal,  $90^\circ$  rotations are satisfied by action above.  $Z_4$  and  $SU(4)$  symmetries constrain spectrum of possible bilinear terms that can emerge in quantum effective action through quantum corrections. A single site mass-term of the form  $\psi^a(x)\psi^a(x)$ , which

is only  $SO(4)$  symmetric, is not allowed by Grassman nature of fermion fields. Another mass term of the form  $\psi^a(x)\psi^b(x)$  breaks not only  $SU(4)$  invariance but also breaks  $Z_4 \rightarrow Z_2$ . Other  $SO(4)$  invariant possible link bilinear operator we can add to our action is

$$O = \sum_{x,\mu} m\varepsilon(x)\xi_\mu(x)\psi^a S_\mu \psi^a \quad (2.4)$$

where symmetric translation operator  $S_\mu$  acts as following  $S_\mu \psi(x) = \psi(x + \mu) + \psi(x - \mu)$ . This operator explicitly breaks lattice *shift* symmetry. Numerical evidence suggests that link-bilinear doesn't survive  $V \rightarrow \infty, m \rightarrow 0$  limit.

## 2.3 Strong coupling expansion

In weak coupling limit  $G \rightarrow 0$  we have massless fermions. Four-fermi coupling is an irrelevant operator by dimensional analysis hence we expect no spontaneous symmetry breaking through fermion bilinear condensation. At strong coupling we can understand system behavior by taking the static limit  $G \rightarrow \infty$  in which we can drop kinetic term. Partition function is completely saturated by four-fermion terms at each site of the form

$$Z \sim [6G^2 \int d\psi^4 d\psi^3 d\psi^2 d\psi^1 \psi^1 \psi^2 \psi^3 \psi^4]^V \quad (2.5)$$

In similar fashion it can argued that no bilinear operator can pick up vev for large  $G$  since that would require only two Grassmann variables to saturate the measure rather than having only four Grassmann variables at each site leading to vanishing vev. To establish that fermions dynamically acquire mass through four-fermion interaction we compute fermion propagator at strong coupling. For convenience we rescale fermions  $\psi \rightarrow \sqrt{\alpha}$  where  $\alpha = \frac{1}{\sqrt{6G}} \ll 1$  which makes

kinetic term pre-factor  $\alpha$  and interaction-term pre-factor unity. Strong coupling expansion now means an expansion in  $\alpha$ . Following the method developed in [22] we consider following fermion two-point function  $\langle \psi^1(x)\psi^1(y) \rangle$  given by

$$\langle \psi^1(x)\psi^1(y) \rangle = \frac{1}{Z} \int D\Psi \psi^1(x)\psi^1(y) e^{-S} \quad (2.6)$$

where  $\int D\Psi = \int \prod_x d\psi^4 d\psi^3 d\psi^2 d\psi^1$ . To saturate Grassman measure at site  $x$  we need to bring down  $\psi^2\psi^3\psi^4$  by expanding  $e^{-S}$ . This leads to following relation

$$\langle \psi^1(x)\psi^1(y) \rangle = \left(\frac{\alpha}{2}\right)^3 \int_x D\Psi \sum_{\mu} \eta_{\mu} [\Psi^1(x+\mu) - \Psi^1(x-\mu)] \psi^1(y) e^{-S} \quad (2.7)$$

where  $\Psi^1 = \varepsilon_{1234}\psi^2\psi^3\psi^4$  and  $\int_x$  implies that integration on site  $x$  can't be done again. Repeating this procedure at site  $x \pm \mu$  we get

$$\langle \psi^1(x)\psi^1(y) \rangle = \left(\frac{\alpha}{2}\right)^3 \sum_{\mu} (\delta_{x+\mu,y} - \delta_{x-\mu,y}) + \left(\frac{\alpha}{2}\right)^4 \int_{x,x+\mu} D\psi \sum_{\mu} [\psi^1(x+2\mu) + \psi^1(x-2\mu)] \psi^1(y) e^{-S} \quad (2.8)$$

It is easy to see that second term on right hand of (2.8) is  $\langle \psi^1(x \pm 2\mu)\psi^1(y) \rangle^1$ . We can express above recurrence relation (2.8) between propagators at displaced sites in a closed form by transforming to momentum space where fermion propagator takes the form

$$\langle \psi^1\psi^1(p) \rangle = \frac{\left(\frac{i}{\alpha}\right) \sum_{\mu} \sin p_{\mu}}{\sum_{\mu} \sin^2 p_{\mu} + m_F^2} \quad (2.9)$$

with  $m_F = -2 + \frac{4}{\alpha^2}$ . An important point here is that mass we get from propagator is a leading order result and doesn't indicate critical  $G$  for which  $m_F \rightarrow 0$ .

An analogous expansion can be performed for bosonic propagator corresponding

---

<sup>1</sup>This expansion with propagator at  $x \pm 2\mu$  is leading order in  $\alpha$ . We can also include contributions from  $x \pm \nu$  which will lead to an expansion with higher order in  $\alpha$

to  $SO(4)$  non-symmetric site bilinear  $B(x) = \psi^1(x)\psi^2(x) + \psi^3(x)\psi^4(x)$

$$\langle B(x)B(y) \rangle = 2\delta_{x,y} + \left(\frac{\alpha}{2}\right)^2 \sum_{\mu,\pm} \langle B(x \pm \mu)B(y) \rangle \quad (2.10)$$

and in momentum space

$$\langle BB(p) \rangle = \frac{\frac{8}{a^2}}{4 \sum_{\mu} \sin^2 p_{\mu} + m_B^2} \quad (2.11)$$

In light of these analytic results we can expect that both fermionic and bosonic spectrum is gapped at strong coupling. Fermionic gap can be understood through condensation of bilinear formed by an elementary fermion  $\psi^a$  and three-fermion composite state  $\Psi^a = \varepsilon_{abcd}\psi^b\psi^c\psi^d$ . Formation of three-fermion composite state is definitely non-perturbative phenomenon only accessible through lattice simulations. Massless phase and massive phases should be separated by a phase transition. Earlier studies of lattice Higgs-Yukawa model using Wilson or staggered fermions revealed PMS(massive) phase at strong coupling however this phase was separated from PMW(massless) phase by an intermediate phase where fermion bilinear condensation spontaneously breaks global symmetries of model under consideration. In these previous models intermediate phase was large enough to make PMS(massive) phase a lattice artifact. Our work will establish that indeed an intermediate phase exists but it's very narrow and can be removed by expanding the phase diagram with an additional parameter.

## 2.4 Auxiliary field representation

Before introducing our generalized Higgs-Yukawa model in next chapter here we present alternative auxiliary field representation of action in (Eq. (2.1)). We employ standard Hubbard-Stratonovich transformation to rewrite action

quadratic in Grassmann variables. For this purpose we introduce auxiliary field  $\sigma_+^{ab}$  which is anti-symmetric in internal indices  $a, b$  and possess important self-dual property.

$$\sigma_{ab}^+ = P_{abcd}^+ \sigma_{cd} = \frac{1}{2} \left( \sigma_{ab} + \frac{1}{2} \varepsilon_{abcd} \sigma_{cd} \right) \quad (2.12)$$

where the projector  $P_{abcd}^\pm$  is given by

$$P_{abcd}^\pm = \frac{1}{2} \left( \delta_{ac} \delta_{bd} \pm \frac{1}{2} \varepsilon_{abcd} \right) \quad (2.13)$$

With these definitions we can write (Eq. (2.1)) as

$$S = \frac{1}{2} \sum_{x, \mu} \psi^a(x) [\eta \cdot \Delta + G \sigma_{ab}^+] \psi^b(x) + \frac{1}{4} \sum_x (\sigma_{ab}^+)^2 \quad (2.14)$$

Fermions can be integrated out to generate Pffafian of fermion operator given by

$$M = \eta \cdot \Delta + G \sigma^+ \quad (2.15)$$

It can shown using local isomorphism  $SO(4) \sim SU_+(2) \times SU_-(2)$  that  $Pf(M)$  is positive definite. Since the operator is real and anti-symmetric it's eigenvalues are pure imaginary and exist in pairs. As  $\sigma_{ab}^+$  is a dynamical field eigenvalues keep changing and for a given  $\sigma_{ab}^+$  configuration having an odd numbers of negative eigenvalues would result in sign problem. Fermions transform as a doublet of  $SU_+(2) \times SU_-(2)$  whereas  $\sigma_{ab}^+$  transforms under  $SU_+(2)$  but it is a singlet under  $SU_-(2)$ . This singlet nature leads to double degeneracy in spectrum of fermion operator as it is invariant under  $SU_-(2)$ . Numerically we can see double degeneracy of eigenvalue spectrum which ensures positivity of Pffafian. This is important for hybrid Monte Carlo algorithm since it eliminates potential sign problem.



## 2.5 Analytic arguments for phase structure

We will examine square of auxiliary field  $\frac{1}{4}\sigma_+^2 = \frac{1}{4}\sum_{a<b}(\sigma_+^{ab})^2$  as a probe for understanding different phases in our numerical work.  $\langle\frac{1}{4}\sigma_+^2\rangle$  has been analytically computed in [3] in  $G \rightarrow 0$  and  $G \rightarrow \infty$  limit. Consider following action

$$S = \frac{1}{2}\sum_{x,\mu}\psi^a(x)[\eta\cdot\Delta + G\sigma_{ab}^+]\psi^b(x) + \frac{\beta}{4}\sum_x(\sigma_{ab}^+)^2 \quad (2.16)$$

It's easy to see that

$$\langle\frac{1}{4}\sigma_+^2\rangle = -\frac{1}{V}\frac{\partial\ln Z(G,\beta)}{\partial\beta} \quad (2.17)$$

By rescaling  $\sigma_+$  with  $\frac{1}{\sqrt{\beta}}$  we can write partition function  $Z(G,\beta)$  as

$$Z(G,\beta) = \int D\sigma_+ \int D\psi e^{-S} = \beta^{-\frac{3V}{2}} Z(\frac{G}{\sqrt{\beta}}, 1) \quad (2.18)$$

where self-dual character of  $\sigma_+$  has been used to allow only three independent integrations at each lattice site. Hence

$$\langle\frac{1}{4}\sigma_+^2\rangle = \frac{3}{2\beta} - \frac{1}{V}\frac{\partial\ln Z(\frac{G}{\sqrt{\beta}}, 1)}{\partial\beta} \quad (2.19)$$

Integrating fermion we have

$$Z(\frac{G}{\sqrt{\beta}}, 1) = \int D\sigma_+ Pf(\eta\cdot\Delta + \frac{G}{\sqrt{\beta}}\sigma_+) e^{-\frac{1}{4}\sigma_+^2} \quad (2.20)$$

For  $G = 0$  partition function is independent of  $\beta$  and second term in (Eq. (2.19)) vanishes. In  $G \rightarrow \infty$  limit  $Z(\frac{G}{\sqrt{\beta}}, 1)$  has simple dependence on  $\beta$  which is  $\beta^{-V}$ . This can be extracted from strong-coupling limit in (Eq. (2.5)). Now setting  $\beta = 1$  after taking the derivative in (Eq. (2.19)) we have

$$\langle \frac{1}{4}\sigma_+^2 \rangle = \begin{cases} \frac{3}{2} & G \rightarrow 0 \\ \frac{5}{2} & G \rightarrow \infty \end{cases} \quad (2.21)$$

In numerical work we have both  $\sigma_+$  and  $\sigma_-$  fields appearing in term quadratic in auxiliary field. Since  $\sigma_-$  doesn't couple with fermions it has no dynamics. Repeating the analysis above for  $\sigma_-$  we can show that  $\langle \frac{1}{4}\sigma_-^2 \rangle = \frac{3}{2}$  completely independent of  $G$ . We will use  $\langle \frac{1}{4}\sigma_+^2 \rangle - \frac{3}{2}$  as an observable rather than  $\langle \frac{1}{4}\sigma_+^2 \rangle$ . We will discuss in next chapter expansion of this model with a kinetic term for auxiliary field and resulting phase diagram.

# Chapter 3

## $SO(4)$ invariant Higgs-Yukawa model on lattice

### 3.1 Introduction

The model presented in this chapter is a generalization of four fermion system with the same symmetries discussed in last chapter. It has received recent attention because of its unusual phase structure comprising massless and massive symmetric phases separated by a very narrow phase in which a small bilinear condensate breaking  $SO(4)$  symmetry is present. The generalization described here simply consists of the addition of a scalar kinetic term. The motivation for this work comes from recent numerical studies [1–8] of a particular lattice four fermion theory constructed using reduced staggered fermions [9]. In three dimensions this theory appears to exist in two phases - a free massless phase and a phase in which the fermions acquire a mass [1, 2, 4, 5]. What is unusual about this is that no local order parameter has been identified which distinguishes between these two phases - the massive phase *does not* correspond to a phase of broken symmetry as would be expected in a conventional Nambu–Jona-Lasinio

scenario. Furthermore, the transition between these two phases is continuous but is not characterized by Heisenberg critical exponents.

When this theory is lifted to four dimensions, however, a very narrow symmetry broken phase reappears characterized by a small bilinear condensate [3, 6–8]. In Ref. [10] we constructed a continuum realization of this lattice theory and argued that topological defects may play an important role in determining the phase structure. This calculation suggests that the addition of a kinetic term for the auxiliary scalar field  $\sigma^+$  used to generate the four fermion interaction may allow access to a single phase transition between massless (paramagnetic weak-coupling, PMW) and massive (paramagnetic strong-coupling, PMS) symmetric phases. In this paper we provide evidence in favor of this from direct numerical investigation of the lattice Higgs-Yukawa model. This development presents the possibility of new critical behavior in a four-dimensional lattice theory of strongly interacting fermions, which would be very interesting from both theoretical and phenomenological viewpoints, and also connects to recent activity within the condensed matter community [11, 12]. In the next section we describe the action and symmetries of the lattice theory, followed by a discussion of analytical results in certain limits in Sec. 3.3. We present numerical results for the phase structure of the theory in Sec. 3.4, and extend this investigation in Sec. 3.5 by adding symmetry-breaking source terms to the action in order to search for spontaneous symmetry breaking in the thermodynamic limit. These investigations reveal significant sensitivity to the hopping parameter  $\kappa$  in the scalar kinetic term, with an antiferromagnetic (AFM) phase separating the PMW and PMS phases for  $\kappa \leq 0$  but an apparently direct and continuous transition between the PMW and PMS phases for a range of positive  $\kappa_1 < \kappa < \kappa_2$ . Our current work constrains  $0 < \kappa_1 < 0.05$  and  $0.085 < \kappa_2 < 0.125$ . We collect these results to present our overall picture for the phase diagram of the theory in Sec. 3.6. We conclude in Sec. 3.7 by summarizing our findings and outlining

future work.

## 3.2 Action and Symmetries

The action we consider takes the form

$$\begin{aligned}
 S = & \sum_x \psi^a [\eta \cdot \Delta^{ab} + G \sigma_{ab}^+] \psi^b + \frac{1}{4} \sum_x (\sigma_{ab}^+)^2 \\
 & - \frac{\kappa}{4} \sum_{x,\mu} [\sigma_{ab}^+(x) \sigma_{ab}^+(x + \mu) + \sigma_{ab}^+(x) \sigma_{ab}^+(x - \mu)]
 \end{aligned}
 \tag{3.1}$$

where repeated indices are to be contracted and  $\eta^\mu(x) = (-1)^{\sum_{i=1}^{\mu-1} x_i}$  are the usual staggered fermion phases. The second line in eqn. 3.1 is essentially a kinetic operator for the  $\sigma^+$  field. With  $\kappa$  set equal to zero we can integrate out the auxiliary field and recover the pure four fermion model studied in Ref. [3]. The rationale for including such a bare kinetic term for the auxiliary field is provided by arguments set out for a related continuum model in Ref. [10]. More concretely, it should be clear that  $\kappa > 0$  favors ferromagnetic ordering of the scalar field and associated fermion bilinear. This is to be contrasted with the preferred antiferromagnetic ordering observed in Refs. [6, 8] for the  $\kappa = 0$  theory.<sup>1</sup> The competition between these two effects raises the possibility that the  $\kappa = 0$  antiferromagnetic fermion bilinear condensate may be suppressed as  $\kappa$  is increased.

In contrast to similar models studied by Refs. [13–21] we fix the coefficient of the  $((\sigma^+)^2 - 1)^2$  term in the action to be  $\lambda = 0$ . Without this term to provide a constraint on the magnitude of the scalar field, we will encounter instabilities when the magnitude of  $\kappa$  is too large. We discuss these instabilities in more

---

<sup>1</sup>Although Ref. [3] observed a strong response to an antiferromagnetic external source, evidence of spontaneous ordering in the zero-source thermodynamic limit was not found until the follow-up Ref. [8].

detail in the next section.

In addition to the manifest  $SO(4)$  symmetry the action is also invariant under a shift symmetry

$$\psi(x) \rightarrow \xi_\rho \psi(x + \rho) \quad (3.2)$$

with  $\xi_\mu(x) = (-1)^{\sum_{i=\mu}^d x_i}$  and a discrete  $Z_2$  symmetry:

$$\sigma^+ \rightarrow -\sigma^+ \quad (3.3)$$

$$\psi^a \rightarrow i\epsilon(x)\psi^a. \quad (3.4)$$

Both the  $Z_2$  and  $SO(4)$  symmetries prohibit local bilinear fermion mass terms from appearing as a result of quantum corrections. Non-local  $SO(4)$ -symmetric bilinear terms can be constructed by coupling fields at different sites in the unit hypercube but such terms break the shift symmetry. Further discussion of possible bilinear mass terms is presented in detail in Ref. [3].

### 3.3 Analytical results

Before we present numerical results we can analyze the model in certain limits. For example, since the action is quadratic in  $\sigma^+$  we can consider the effective action obtained by integrating over  $\sigma^+$ . The scalar part of the action may be rewritten

$$\frac{1}{4}\sigma^+ (-\kappa\Box + m^2) \sigma^+ \quad (3.5)$$

where  $m^2 = (1 - 2d\kappa)$  is an effective mass squared for the  $\sigma^+$  field in  $d$  dimensions and  $\Box$  is the usual discrete scalar laplacian. Integrating out  $\sigma^+$  yields an effective action for the fermions

$$S = \sum \psi(\eta.\Delta) \psi - G^2 \sum \Sigma^+ [-\kappa\Box + m^2]^{-1} \Sigma^+ \quad (3.6)$$

where  $\Sigma_{ab}^+ = [\psi_a \psi_b]_+$  is the self-dual fermion bilinear. For  $\kappa$  small we can expand the inverse operator in powers of  $\kappa/m^2$  and find

$$S = \sum \psi (\eta \cdot \Delta) \psi - \frac{G^2}{m^2} \Sigma^+ \left( \mathbb{I} + \frac{\kappa}{m^2} \square + \dots \right) \Sigma^+. \quad (3.7)$$

To leading order the effect of non-zero  $\kappa$  is to renormalize the Yukawa coupling  $G \rightarrow \frac{G}{m} = \frac{G}{\sqrt{1-2\kappa d}}$ . At next to leading order we obtain the term

$$\frac{G^2}{m^4} \sum \Sigma^+ [-\kappa \square] \Sigma^+. \quad (3.8)$$

For  $\kappa > 0$  and sufficiently large  $G$  this term favors a ferromagnetic ordering of the fermion bilinear  $\langle \Sigma^+ \rangle \neq 0$ . Conversely it suggests an antiferromagnetic ordering with  $\langle \epsilon(x) \Sigma^+(x) \rangle \neq 0$  for  $\kappa < 0$ . This can be seen more clearly if one rewrites the action in the alternative form

$$S = \sum \psi (\eta \cdot \Delta) \psi - G^2 \sum \Sigma^+ [-\kappa B + \mathbb{I}]^{-1} \Sigma^+ \quad (3.9)$$

where  $B\Sigma = \sum_{\mu} [\Sigma(x + \mu) + \Sigma(x - \mu)]$ . Clearly changing the sign of  $\kappa$  can be compensated by transforming  $\Sigma^+ \rightarrow \epsilon(x) \Sigma^+$  since  $\epsilon(x)$  anticommutes with  $B$ . Two of us investigated the case  $\kappa = 0$  in Ref. [8] and observed a narrow phase with antiferromagnetic ordering. Since  $\kappa > 0$  produces ferromagnetic terms we expect the tendency toward antiferromagnetic ordering to be reduced as  $\kappa$  is increased. The numerical results described in the following section confirm this.

For  $\kappa > \frac{1}{2d} = \frac{1}{8}$  the squared mass changes sign and one expects an instability to set in with the model only being well defined for  $\kappa < \frac{1}{8}$ . Actually there is also a lower bound on the allowed values of  $\kappa$ . To see this return to eqn. 3.5 and

perform the change of variables

$$\begin{aligned}\sigma_{ab}^+(x) &\rightarrow \epsilon(x)\sigma_{ab}^+(x) \\ \kappa &\rightarrow -\kappa.\end{aligned}\tag{3.10}$$

This implies that the partition function  $Z(\kappa)$  is an even function of  $\kappa$  at  $G = 0$ . We can show that this is also true in the strong coupling limit  $G \rightarrow \infty$ . In this limit we can drop the fermion kinetic term from the action in eqn. 3.1 and expand the Yukawa term in powers of the fermion field

$$Z = \int D\psi D\sigma^+ \left( 1 - G\psi\sigma^+\psi + \frac{1}{2}(G\psi\sigma^+\psi)^2 \right) e^{S(\sigma^+)}.\tag{3.11}$$

The only terms that survive the Grassmann integrations contain even powers of  $\sigma^+$ . Using the same transformation eqn. 3.10 allows us to show that the partition function is once again an even function of  $\kappa$ . Thus we expect that at least for weak and strong coupling the partition function is only well defined in the strip  $-\frac{1}{8} < \kappa < \frac{1}{8}$ .

It is also instructive to compute the effective action for the scalar fields having integrated out the fermions. This takes the form<sup>2</sup>

$$S_{\text{eff}} = -\frac{1}{4}\text{Tr} \ln \left( -\Delta_\mu^2 + M^2 + G\eta_\mu(x)\epsilon(x)\Delta_\mu\sigma^+ \right)\tag{3.12}$$

where  $M^2 = -G^2(\sigma^+)^2$ . To zeroth order in derivatives the resultant effective potential is clearly of symmetry breaking form. The first non-trivial term in the

---

<sup>2</sup>To facilitate the computation we have traded the original ferromagnetic Yukawa coupling  $\psi\sigma^+\psi$  in eqn. 3.1 for an antiferromagnetic coupling  $\epsilon(x)\psi\sigma^+\psi$  while simultaneously trading  $\kappa \rightarrow -\kappa$  as in eqn. 3.10. This allows us to simplify the expression for the effective action by using the fact that  $\epsilon(x)$  anticommutes with  $\Delta_\mu$ .



derivative or large mass  $M$  expansion of this action is

$$-\frac{G^2}{8M^4} \sum (\Delta_\mu \sigma^+)^2. \quad (3.13)$$

Thus even the pure four fermion model will produce kinetic terms for the scalar field through loop effects confirming the need to include such terms in the classical action.<sup>3</sup> In Ref. [10] it was argued that an additional term should also be generated which is quartic in derivatives in the continuum limit. This term *only* arises for a self-dual scalar field and leads to the possibility that topological field configurations called Hopf defects may play a role in understanding the massive symmetric phase.

### 3.4 Phase Structure

One useful observable we can use to probe the phase structure in the  $(\kappa, G)$  plane is  $\langle \sigma_+^2 \rangle$ . This is shown for three different values of  $\kappa$  on a  $8^4$  lattice in Fig. 3.1. At  $\kappa = 0$  this observable served as a proxy for the four fermion condensate and we observe this to be the case also when  $\kappa \neq 0$ . Thus we see that a four fermion phase survives at strong Yukawa coupling  $G$  even for non-zero values of  $\kappa$ .

Of course the key issue is what happens for intermediate values of  $G$ . At  $\kappa = 0$  a narrow intermediate phase was observed for  $0.95 \lesssim G \lesssim 1.15$  in two different ways: from the volume scaling of a certain susceptibility [6] and by examining fermion bilinear condensates as functions of external symmetry

---

<sup>3</sup>A similar argument suggests that a quartic term  $\lambda((\sigma^+)^2 - 1)^2$  will also be produced. As mentioned in the previous section we fix  $\lambda = 0$  in the calculations reported here. In addition to simplifying the parameter space to be considered, this step is also motivated by observations [20, 21] that  $\lambda$  seems to have little effect on the large-scale features of the phase diagram in similar Higgs-Yukawa models.

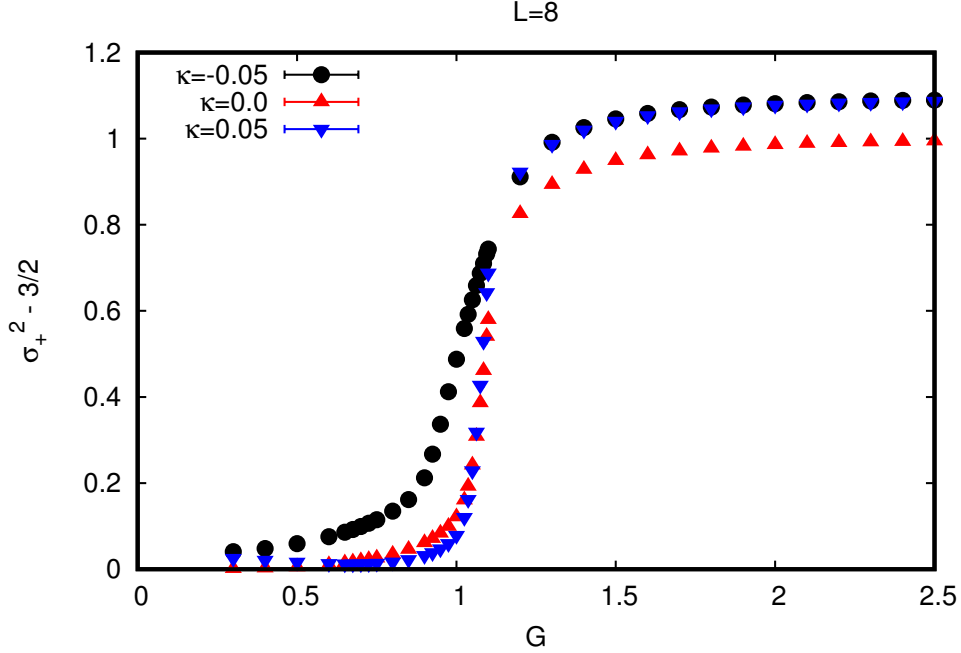


Figure 3.1:  $\langle \sigma_+^2 \rangle$  vs  $G$  for  $L = 8$ , comparing  $\kappa = \pm 0.05$  and 0.

breaking sources [8]. This susceptibility is defined as

$$\chi_{\text{stag}} = \frac{1}{V} \sum_{x,y,a,b} \langle \epsilon(x) \psi^a(x) \psi^b(x) \epsilon(y) \psi^a(y) \psi^b(y) \rangle \quad (3.14)$$

where  $V = L^4$  and the subscript “<sub>stag</sub>” refers to the presence of the parity factors  $\epsilon(x)$  associated with antiferromagnetic ordering. It is shown in Fig. 3.2 for three different lattice volumes at  $\kappa = 0$ . The linear dependence of the peak height on the lattice volume is consistent with the presence of a condensate  $\langle \epsilon(x) \psi^a(x) \psi^b(x) \rangle \neq 0$ .

Since  $\kappa < 0$  generates additional antiferromagnetic terms in the effective fermion action we expect this bilinear phase to survive in the  $\kappa < 0$  region of the phase diagram. This is confirmed in our calculations. Figure 3.3 shows a similar susceptibility plot for  $\kappa = -0.05$ , in which the width of the broken phase *increases* while the peak height continues to scale linearly with the volume indicating the

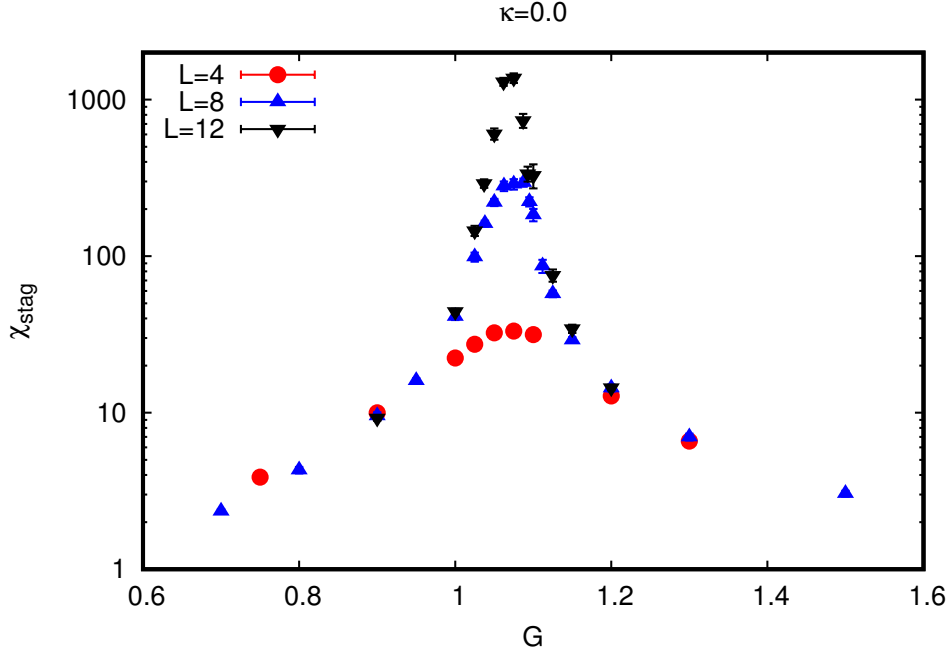


Figure 3.2:  $\chi_{\text{stag}}$  vs  $G$  at  $\kappa = 0$  for  $L = 4, 8$  and  $12$ .

presence of an antiferromagnetic bilinear condensate.

The situation changes for  $\kappa > 0$ . Fig. 3.4 shows the susceptibility  $\chi_{\text{stag}}$  for  $\kappa = 0.05$ . While a peak is still observed for essentially the same value of  $G$  the height of this peak no longer scales with the volume. Since  $\kappa > 0$  induces ferromagnetic terms in the action we also examine the associated ferromagnetic susceptibility

$$\chi_{\text{f}} = \frac{1}{V} \sum_{x,y,a,b} \langle \psi^a(x) \psi^b(x) \psi^a(y) \psi^b(y) \rangle. \quad (3.15)$$

This is plotted in Fig. 3.5 for  $\kappa = 0.05$ , which shows no evidence of ferromagnetic ordering at this value of  $\kappa$ . In the appendix we show that  $\kappa = 0.1$  is sufficiently large to produce a ferromagnetic phase.

The lack of scaling of the  $\chi_{\text{stag}}$  peak with volume at  $\kappa = 0.05$  might suggest that the system is no longer critical at this point. This is not the case. Figure 3.6 shows the number of conjugate gradient (CG) iterations needed for Dirac op-

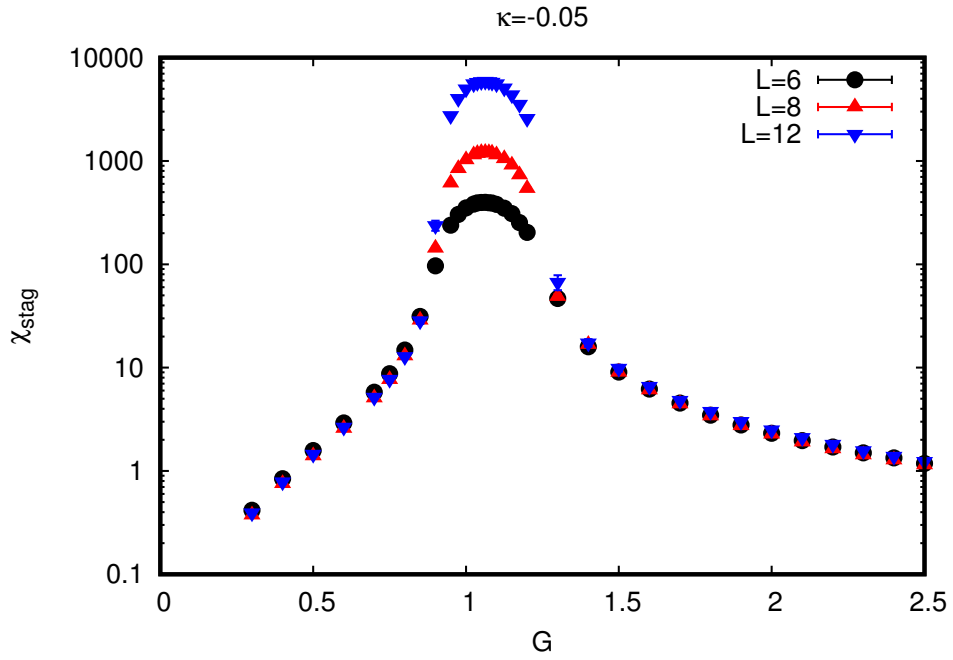


Figure 3.3:  $\chi_{\text{stag}}$  vs  $G$  at  $\kappa = -0.05$  for  $L = 6, 8$  and  $12$ .

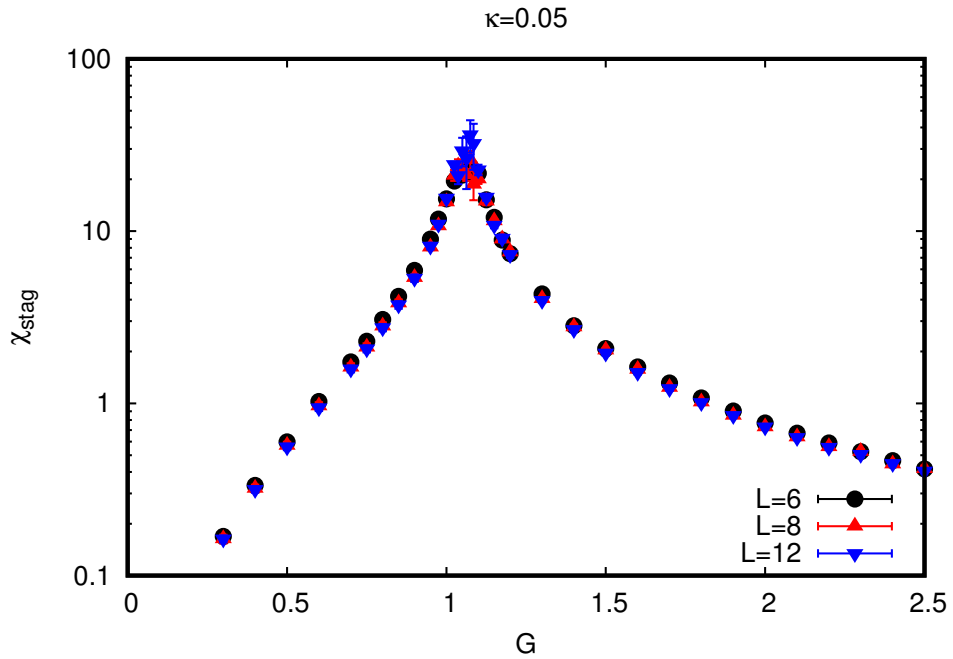


Figure 3.4:  $\chi_{\text{stag}}$  vs  $G$  at  $\kappa = 0.05$  for  $L = 6, 8$  and  $12$ .

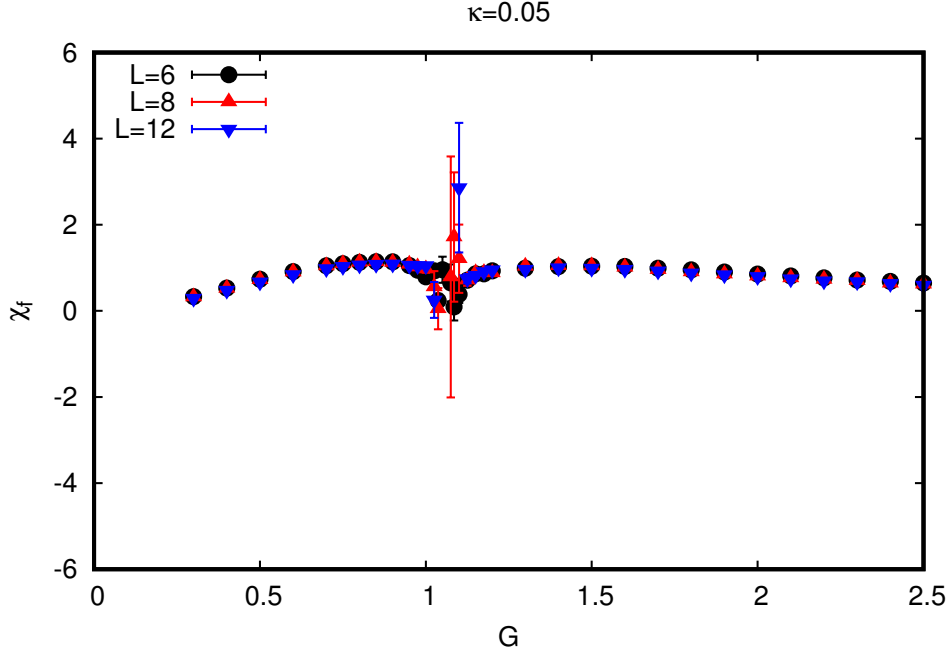


Figure 3.5: The ferromagnetic susceptibility  $\chi_f$  vs  $G$  at  $\kappa = 0.05$  for  $L = 6, 8$  and  $12$ . Unlike the other susceptibility plots, the y-axis scale is not logarithmic.

erator inversions at  $\kappa = 0$  and  $\kappa = 0.05$  as a function of  $G$  for  $L = 8$ . This quantity is a proxy for the fermion correlation length in the system. The peak at  $\kappa = 0.05$  is significantly greater than at  $\kappa = 0$ . Furthermore we have observed that it increases strongly with lattice size rendering it very difficult to run computations for  $L \geq 16$ . Our conclusion is that there is still a phase transition around  $G \approx 1.05$  for small positive  $\kappa$  but no sign of a bilinear condensate. We will reinforce this conclusion in the next section where we will perform an analysis of bilinear vevs versus external symmetry breaking sources.

It is interesting to investigate the phase diagram away from the critical region. Figure 3.7 shows the four fermion condensate vs  $\kappa$  at  $G = 2$ , which vanishes at  $|\kappa| = \frac{1}{8}$  as expected by stability arguments. The structure of the curve suggests that there may be a phase transition at  $\kappa \approx 0.085$  from a four fermion condensate to a ferromagnetic condensate. This is illustrated by Fig. 3.8 where

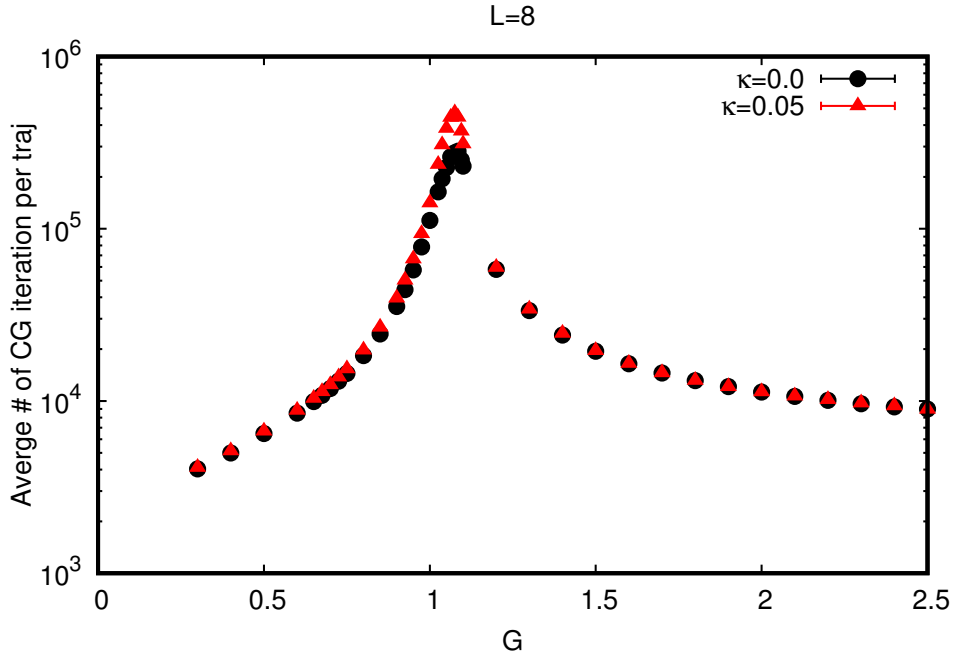


Figure 3.6: Average number of CG iterations for Dirac operator inversions on  $L = 8$  lattices, plotted vs  $G$  for  $\kappa = 0$  and  $0.05$ .

for  $\kappa > 0$  we show the magnetization

$$M = \frac{1}{V} \left\langle \left| \sum_x \sum_{a < b} \sigma_{ab}^+(x) \right| \right\rangle. \quad (3.16)$$

The behavior near  $\kappa \approx -0.085$  in Fig. 3.8 shows a similar transition from four fermion condensate to antiferromagnetic phase. For  $\kappa < 0$  we add the usual parity factor  $\epsilon(x)$  to define the staggered magnetization  $M_s$ .

### 3.5 Fermion Bilinears

In this section we add source terms to the action that explicitly break both the  $SO(4)$  and  $Z_2$  symmetries and, by examining the volume dependence of various bilinear vevs as the sources are sent to zero, address the question of whether

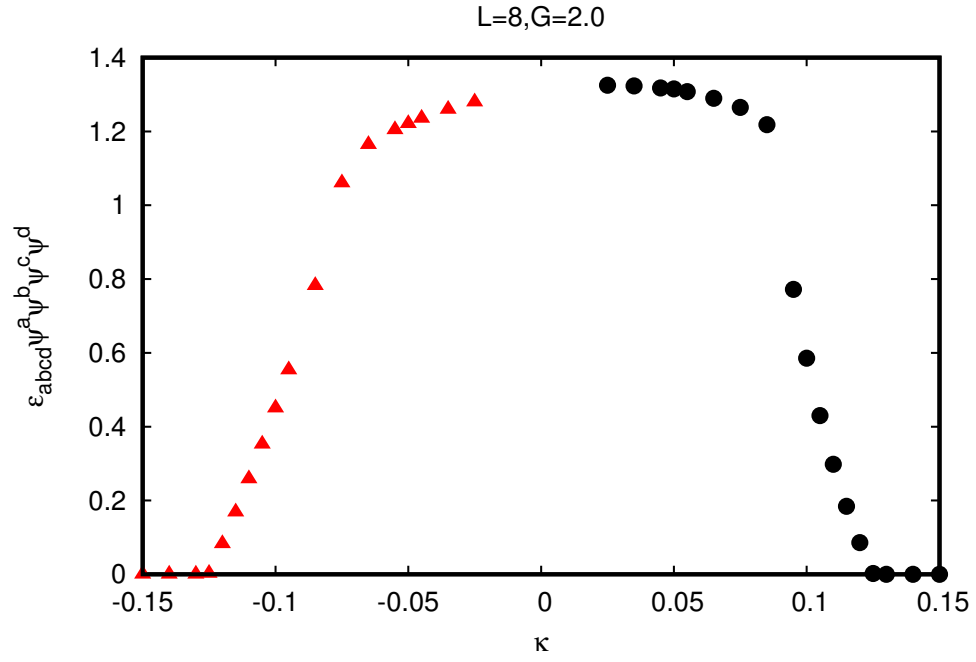


Figure 3.7: Four fermion condensate at  $G = 2$  vs  $\kappa$  for  $L = 8$ .

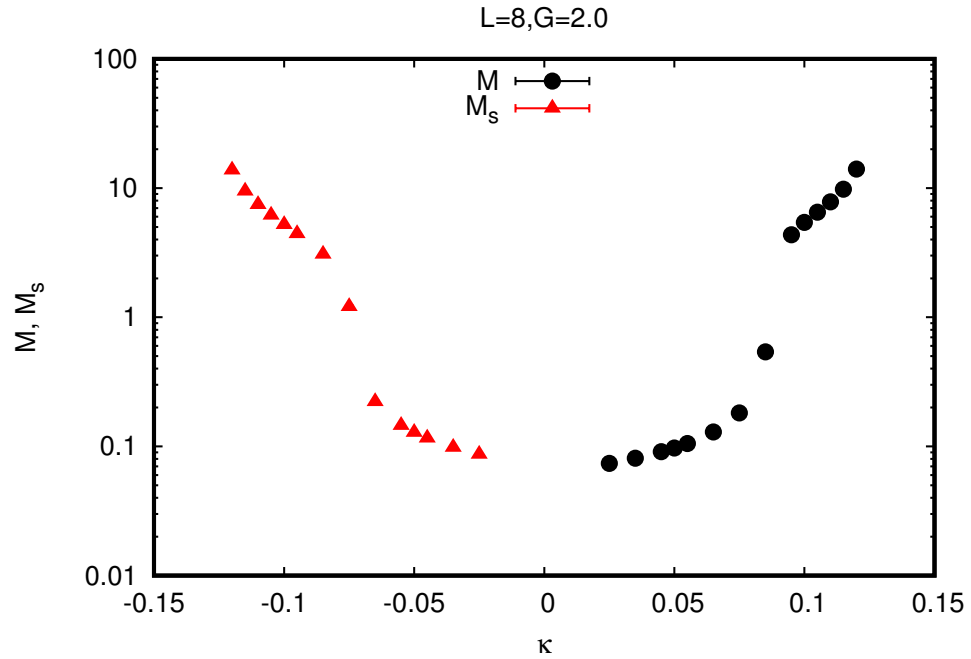


Figure 3.8: Ferromagnetic and staggered magnetizations at  $G = 2$  vs  $\kappa$  for  $L = 8$ .

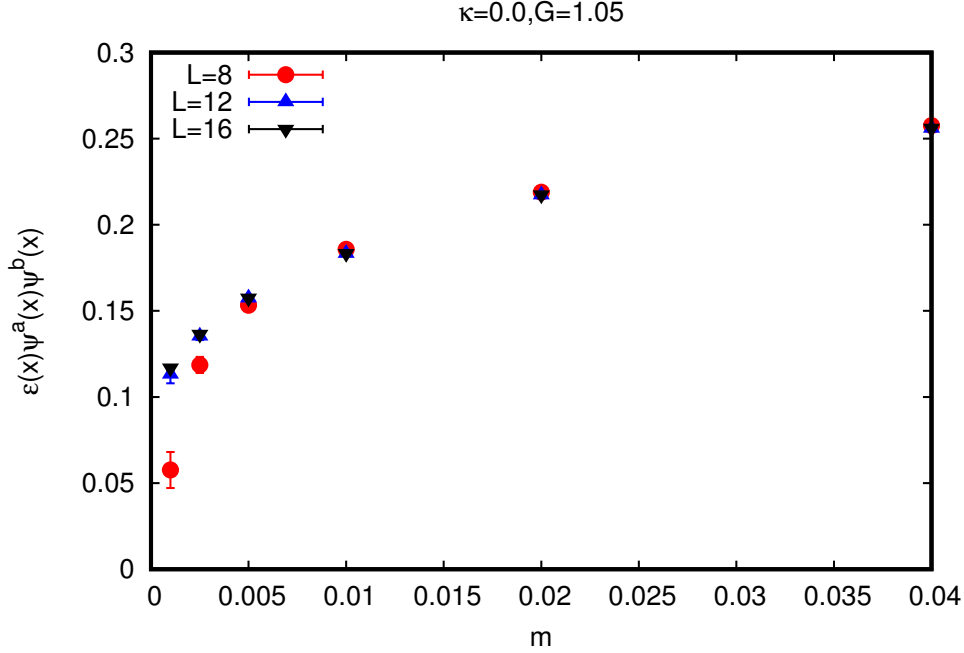


Figure 3.9: Antiferromagnetic bilinear condensate vs  $m_2$  (with  $m_1 = 0$ ) at  $(\kappa, G) = (0, 1.05)$  for  $L = 8, 12$  and  $16$ .

spontaneous symmetry breaking occurs in the system. The source terms take the form

$$\delta S = \sum_{x,a,b} (m_1 + m_2 \epsilon(x)) [\psi^a(x) \psi^b(x)] \Sigma_+^{ab} \quad (3.17)$$

where the  $SO(4)$  symmetry breaking source  $\Sigma_+^{ab}$  is

$$\Sigma_+^{ab} = \begin{pmatrix} i\sigma_2 & 0 \\ 0 & i\sigma_2 \end{pmatrix}. \quad (3.18)$$

For  $\kappa = 0$  we find evidence in favor of antiferromagnetic ordering consistent with the volume scaling of the susceptibility  $\chi_{\text{stag}}$ . The antiferromagnetic bilinear vev  $\langle \epsilon(x) \psi^a(x) \psi^b(x) \rangle$  plotted in Fig. 3.9 (with  $m_1 = 0$ ) picks up a non-zero value in the limit  $m_2 \rightarrow 0, L \rightarrow \infty$  signaling spontaneous symmetry breaking. The data correspond to runs at the peak in the susceptibility  $G = 1.05$ , and similar results are found throughout the region  $0.95 \lesssim G \lesssim 1.15$ . This confirms the presence



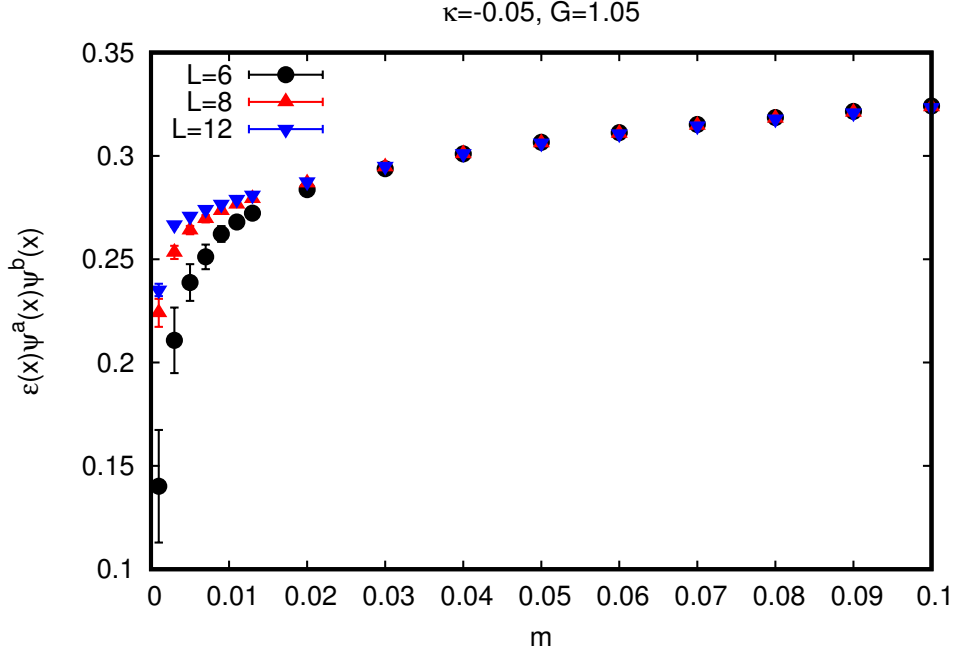


Figure 3.10: Antiferromagnetic bilinear condensate vs  $m_2 = m_1$  at  $(\kappa, G) = (-0.05, 1.05)$  for  $L = 6, 8$  and  $12$ .

of the condensate inferred from the linear volume scaling of the susceptibility reported in the previous section.

For  $\kappa < 0$  the picture is similar with Fig. 3.10 showing the same vev vs  $m_2 = m_1$  for  $\kappa = -0.05$  at the same  $G = 1.05$ . (Recall from Figs. 3.2–3.4 that the center of the peak in  $\chi_{\text{stag}}$  moves only very slowly for  $|\kappa| \leq 0.05$ .) The increase in vev with larger volumes at small  $m_2$  is again very consistent with the presence of a non-zero condensate in the thermodynamic limit. The magnitude of this condensate at  $\kappa = -0.05$  is clearly larger than at  $\kappa = 0$ .

The situation for  $\kappa > 0$  is quite different. Figure 3.11 shows plots of both antiferromagnetic and ferromagnetic bilinear vevs at  $(\kappa, G) = (0.05, 1.05)$  for several lattice volumes. These plots show no sign of a condensate as the source terms are removed in the thermodynamic limit. Broken phases thus seem to be evaded for small  $\kappa > 0$ . In the appendix we include results for larger  $\kappa \geq 0.085$ .

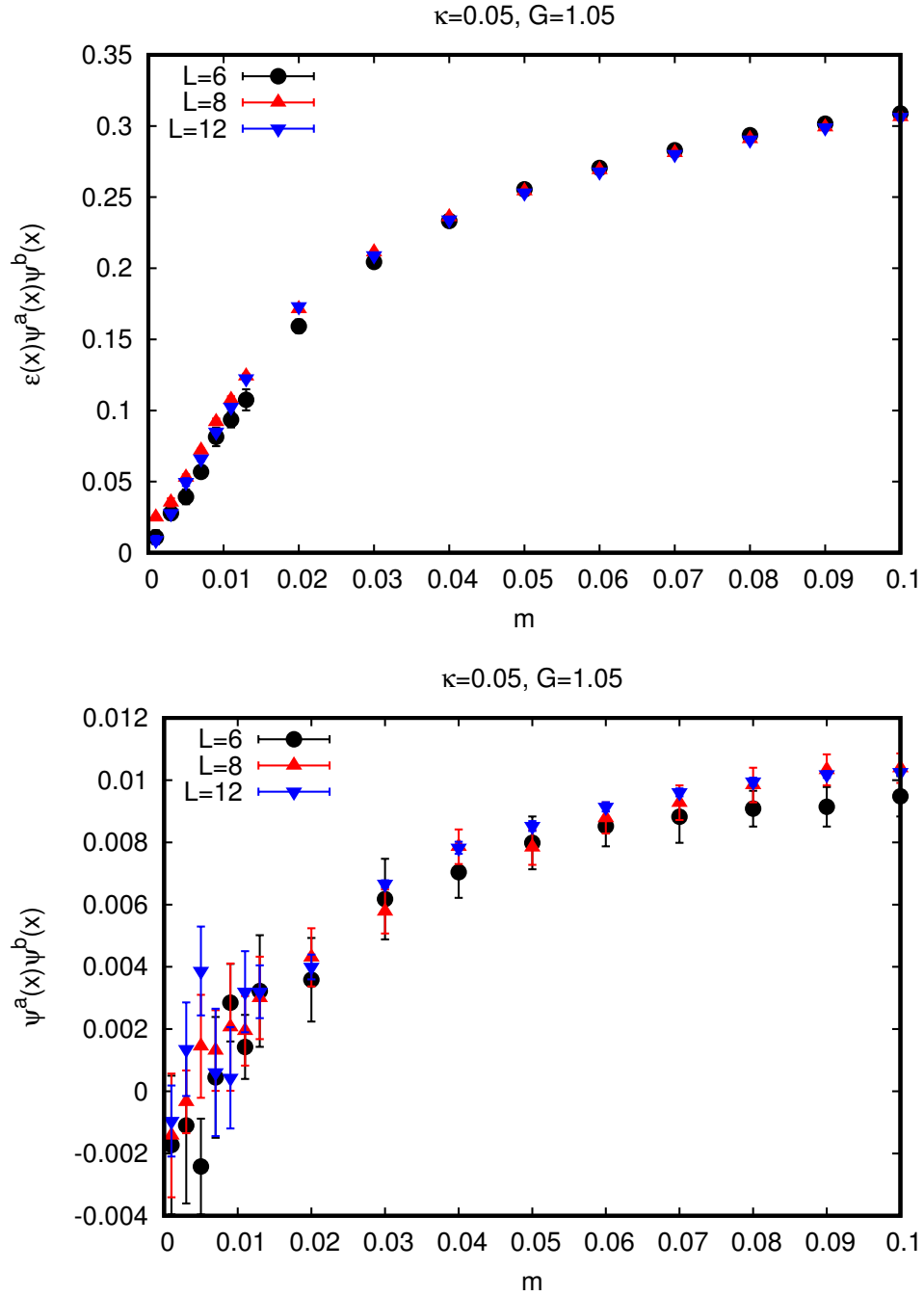


Figure 3.11: Antiferromagnetic (left) and ferromagnetic (right) bilinear condensates vs  $m_2 = m_1$  at  $(\kappa, G) = (0.05, 1.05)$  for  $L = 6, 8$  and  $12$ .

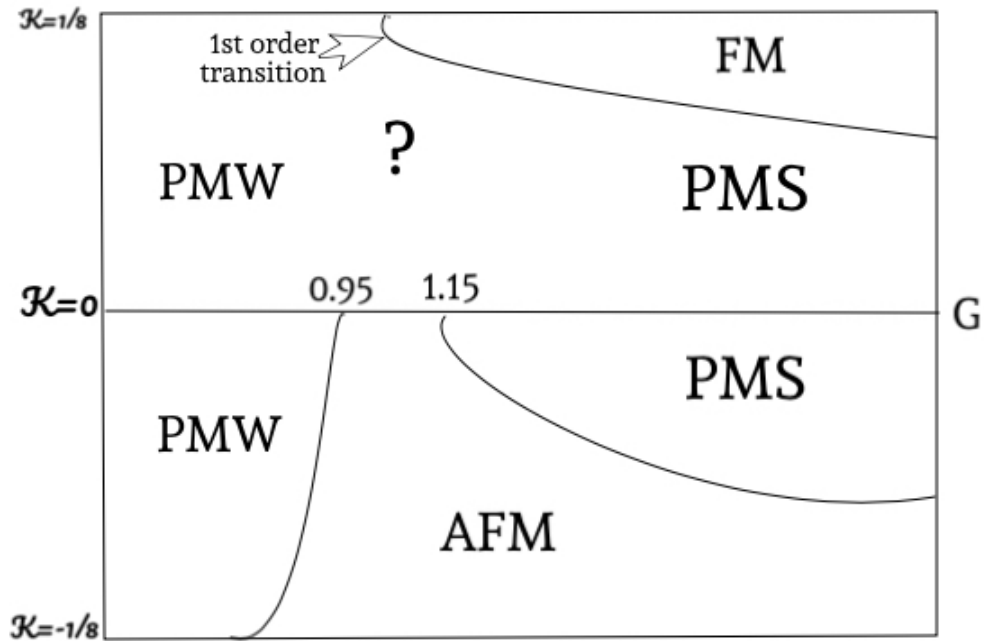


Figure 3.12: Sketch of the phase diagram in the  $(\kappa, G)$  plane.

While we observe a similar absence of bilinear condensates at  $\kappa = 0.085$ , the expected ferromagnetic phase does clearly appear for  $\kappa \approx 0.1$  and we are able to set loose bounds on the range  $\kappa_1 < \kappa < \kappa_2$  within which there appears to be a direct PMW–PMS transition, namely  $0 < \kappa_1 < 0.05$  while  $0.085 < \kappa_2 < 0.125$ .

### 3.6 Resulting phase diagram

Putting this all together we sketch the phase diagram in Fig. 3.12. For small  $G$  the system is disordered and the fermions massless. For large  $G$  and small  $\kappa$  we see a four fermion condensate as before. As  $\kappa$  increases in magnitude one expects a transition to either a ferromagnetic ( $\kappa > 0$ ) or antiferromagnetic ( $\kappa < 0$ ) phase for sufficiently large  $G$ . However, for small positive  $\kappa$  close to  $G = 1.05$ , while we observe no sign of a bilinear condensate there are strong indications of critical slowing down and a large fermion correlation length. Since

the weak and strong coupling phases *cannot* be analytically connected (one is massless while in the other the fermions acquire a mass) there must be at least one phase transition between them. Unlike the situation for  $\kappa \leq 0$  we see no evidence for an intermediate broken-symmetry phase in this region and hence the simplest conclusion is that a single phase transition separates the two symmetric phases. Thus far we have seen no sign of first order behavior so this transition appears to be continuous.

### 3.7 Summary and Conclusions

In this chapter we have expanded on our investigations of the phase diagram of a four-dimensional lattice Higgs-Yukawa model comprising four reduced staggered fermions interacting with a scalar field transforming in the self-dual representation of a global  $SO(4)$  symmetry. This extends recent work on a related four fermion model in which a massless symmetric phase is separated from a massive symmetric phase by a narrow broken symmetry phase characterized by a small antiferromagnetic bilinear fermion condensate [3, 6–8].

Our main result is evidence that this broken phase may be eliminated in the generalized phase diagram by tuning the hopping parameter in the scalar kinetic term. This should not be too surprising since the ferromagnetic ordering favored by  $\kappa > 0$  counteracts the antiferromagnetic ordering observed for  $\kappa \leq 0$ . There is then a range of positive  $\kappa_1 < \kappa < \kappa_2$  throughout which the massless and massive symmetric phases appear to be separated by a single phase transition. Since no order parameter distinguishes the two phases this transition is not of a conventional Landau-Ginzburg type. Ref. [10] argues in a related continuum model that the transition may be driven instead by topological defects. It would be fascinating to investigate whether these topological defects could be seen in numerical calculations.

Future work will also focus on better constraining the values of  $\kappa_1$  and  $\kappa_2$  between which we observe the direct PMW–PMS transition. Our current results suffice to establish that these two points are well separated,  $0 < \kappa_1 < 0.05$  while  $0.085 < \kappa_2 < 0.125$ , but neither is very precisely determined yet. It is also important to measure more observables in order to search for non-trivial scaling behavior associated with this transition. The lack of scaling that we observe for the susceptibility  $\chi_{\text{stag}}$  at the phase boundary in Fig. 3.4 currently suggests that the scaling dimension of the bilinear fermion operator would be greater than two at any putative new critical point.

Clearly the possibility of realizing new fixed points in strongly interacting fermionic systems in four dimensions is of great interest and we hope our results stimulate further work in this area. Another important direction is constructing EP-like model with addition of generalized Wilson term of Yukawa type with auxiliary field  $\sigma_{ab}^+$  and explore the region of phase diagram where we see a continuous transition from massless to massive fermions. This is discussed in detail in Appendix B of this chapter. Moreover we construct continuum realization of our model which is going to be subject of next chapter.

## 3.8 Appendix A

In this appendix we collect some additional results for larger  $\kappa > 0.05$ , both to strengthen our conclusions that there is no bilinear phase for a range of positive  $\kappa$  and to confirm that a ferromagnetic phase does appear once  $\kappa$  and  $G$  are sufficiently large. First, in Fig. 3.13 we consider  $\kappa = 0.085$ , around the potential transition identified in Figs. 3.7 and 3.8. Whereas those earlier figures considered  $G = 2$ , here we use the same  $G = 1.05$  as Fig. 3.11 for  $\kappa = 0.05$ . We again observe an absence of spontaneous symmetry breaking, with the antiferromagnetic and ferromagnetic bilinear condensates both vanishing as the symmetry-breaking source terms are removed, with no visible dependence on the lattice volume.

The situation is qualitatively different in Fig. 3.14, which considers  $\kappa = 0.1$  (at  $G = 1.1$ ) and shows clear signs of a non-zero ferromagnetic condensate in the  $L \rightarrow \infty$  limit. In Fig. 3.15 we compare the ferromagnetic susceptibility  $\chi_f$  for three different  $\kappa = 0, 0.05$  and  $0.1$ . While this susceptibility is uniformly small for  $\kappa = 0$  and  $0.05$ , the larger  $\kappa = 0.1$  produces a strong jump to a large value for  $G \gtrsim 1.1$ , suggesting a first-order transition into the ferromagnetic phase.

Finally, Fig. 3.16 compares the four-fermion condensate vs  $G$  for  $\kappa = 0.05$  and  $0.1$ . Although the larger value of  $\kappa$  significantly reduces the four-fermion condensate for large  $G \gtrsim 1.2$  (as previously shown in Fig. 3.7), there is a very narrow peak around  $G \approx 1.05$ . This may suggest that the system still transitions directly from the PMW phase into the PMS phase before undergoing a second transition into the ferromagnetic phase. We are therefore not yet able to set tighter constraints than  $0.085 < \kappa_2 < 0.125$  on the upper boundary of the direct PMW–PMS transition. This region of the phase diagram appears rather complicated, though Fig. 3.15 makes it clear that the ferromagnetic phase persists to large  $G$  rather than being a narrow intermediate phase of the sort

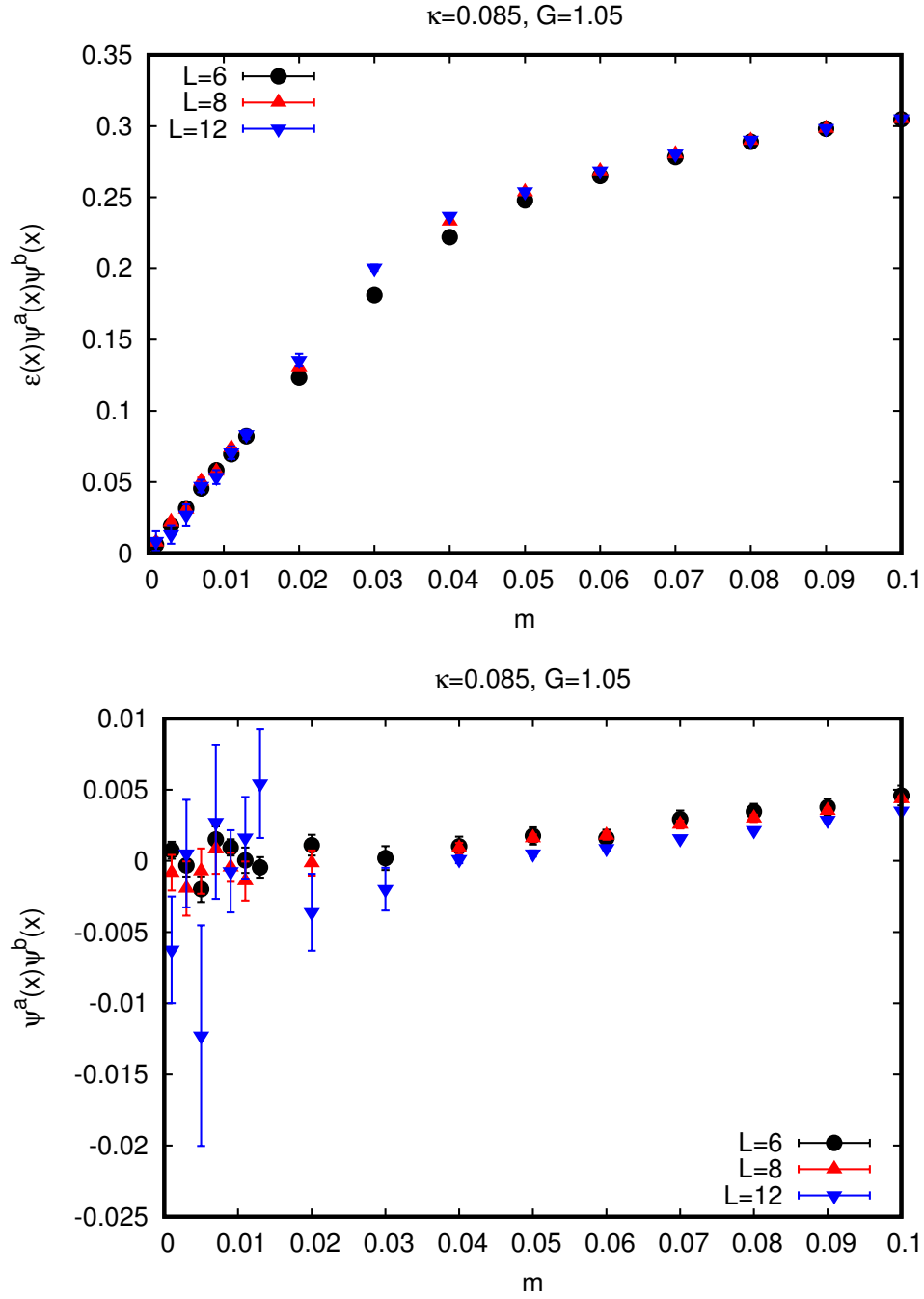


Figure 3.13: Antiferromagnetic (left) and ferromagnetic (right) bilinear condensates vs  $m_2 = m_1$  at  $(\kappa, G) = (0.085, 1.05)$  for  $L = 6, 8$  and  $12$ .

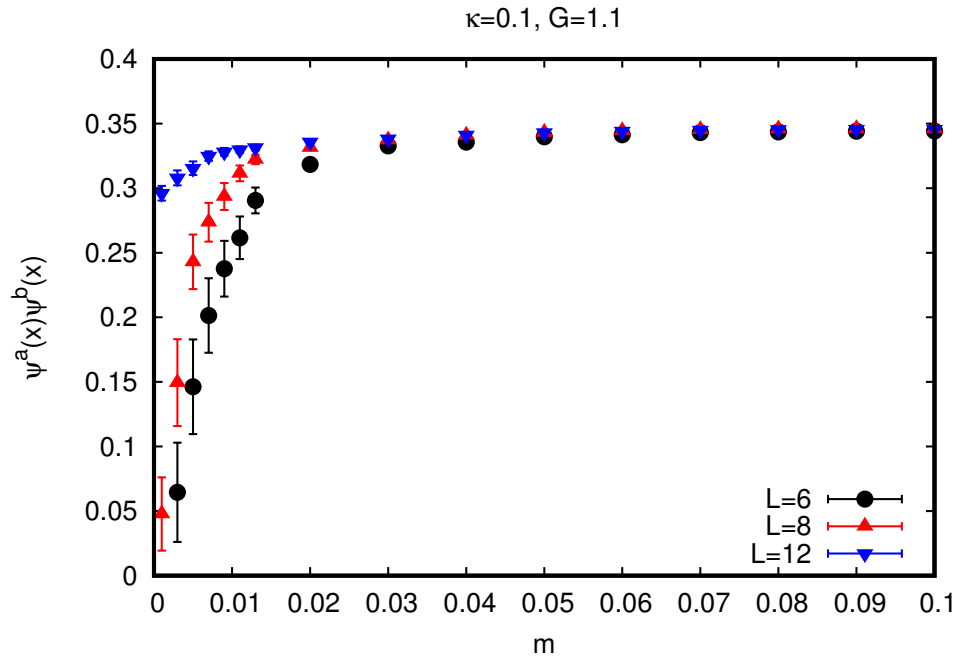


Figure 3.14: Ferromagnetic bilinear condensate vs  $m_2 = m_1$  at  $(\kappa, G) = (0.1, 1.1)$  for  $L = 6, 8$  and  $12$ .

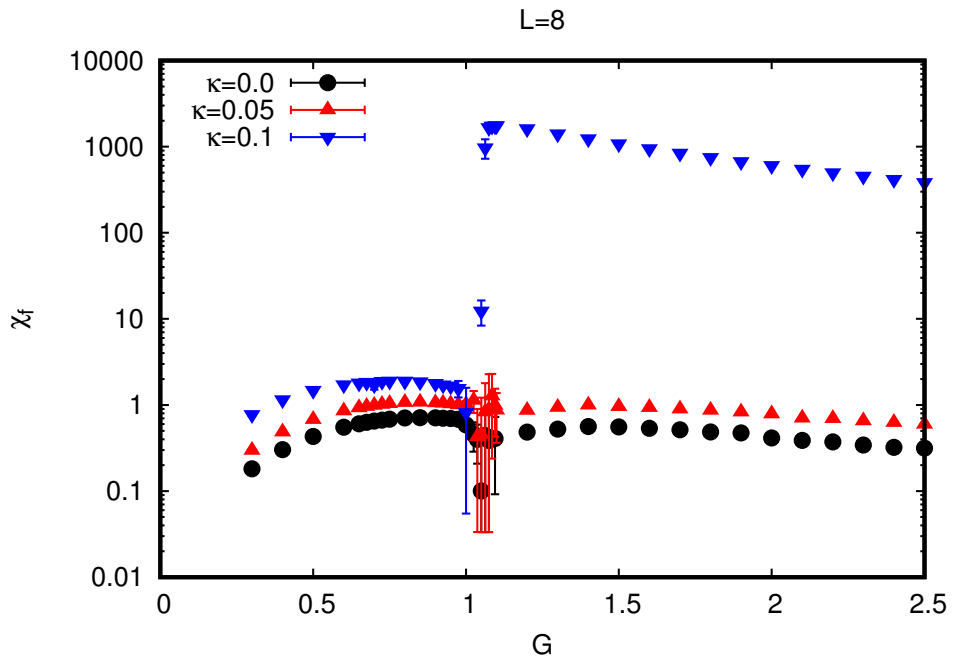


Figure 3.15: The  $L = 8$  ferromagnetic susceptibility  $\chi_f$  vs  $G$  for  $\kappa = 0, 0.05$  and  $0.1$ .



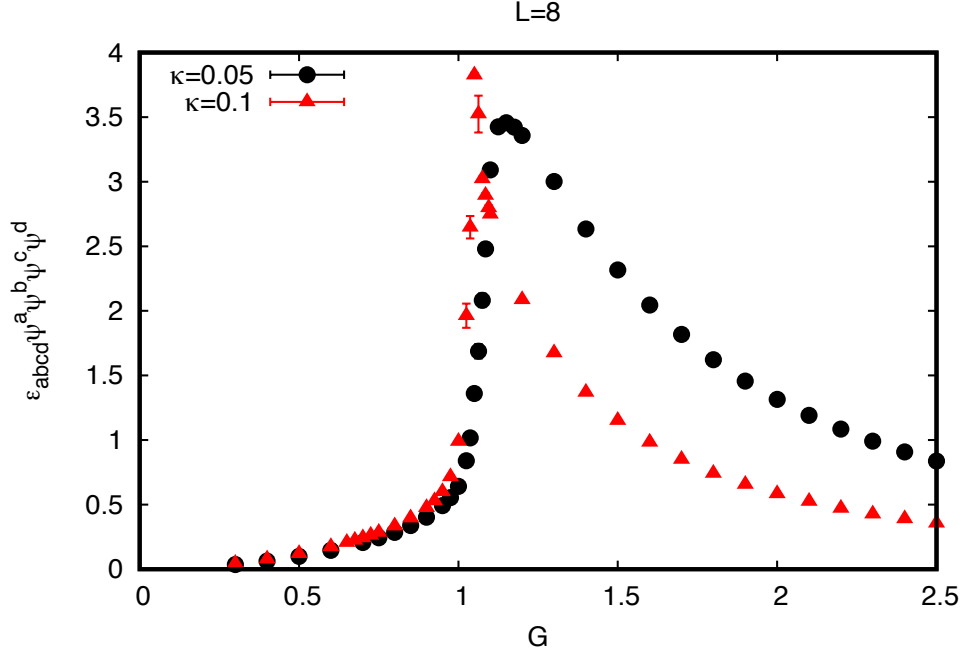


Figure 3.16: Four fermion condensate on vs  $G$  for  $L = 8$ , comparing  $\kappa = 0.5$  and  $0.1$ .

we see for  $\kappa \leq 0$ . This is reflected in our sketch of the phase diagram, Fig. 3.12.

### 3.9 Appendix B

In this appendix we discuss Eichten-Prekill proposal of gapping out mirror fermions using auxiliary interactions which are irrelevant in the continuum limit. We use reduced staggered formalism and show that the propagator with generalized Wilson term has the right pole structure which in the continuum only realizes a single specie of fermion and all doubler modes become infinitely massive. We start with the action studied in [3] and add generalized Wilson term to this action.

$$S = \sum_x \psi^a(x)[\eta.\Delta]\delta^{ab}\psi^b(x) + \sum_x \frac{G}{2}\sigma_+^{ab}\Sigma_+^{ab} + \frac{r}{2}\sum_x \sigma_+^{ab}(x)[\psi^a(x)\square\psi^b(x)]_+ + \frac{1}{4}\sum_x (\sigma_+^{ab})^2 \quad (3.19)$$

We integrate out the auxiliary field to generate action containing only Grassmann variables.

$$S = \sum_x \psi^a(x)[\eta.\Delta]\delta^{ab}\psi^b(x) + \frac{G^2}{4}\sum_x \epsilon_{abcd}\psi^a(x)\psi^b(x)\psi^c(x)\psi^d(x) + \frac{r^2}{4}\sum_x [\psi^a(x)\square\psi^b(x)]_+^2 + \sum_x \frac{rG}{2}\Sigma_+^{ab}(x)[\psi^a(x)\square\psi^b(x)]_+ \quad (3.20)$$

We start with simplifying last two terms in action

$$\Sigma_+^{ab}(x)[\psi^a(x)\square\psi^b(x)]_+ = \sum_{\mu,\pm} 2\epsilon_{abcd}[\psi^a(x)\psi^b(x)\psi^c(x)\psi^d(x\pm\mu) - \psi^a(x)\psi^b(x)\psi^c(x)\psi^d(x)] \quad (3.21)$$

$$[\psi^a(x)\square\psi^b(x)]_+^2 = ([\psi^a(x)\psi^b(x+\mu)]_+ + [\psi^a(x)\psi^b(x-\mu)]_+ - 2\Sigma_+^{ab})^2 \quad (3.22)$$

By expanding and simplifying using Grassmann nature of these fields we have

$$S = \sum_x \psi^a(x)[\eta.\Delta]\delta^{ab}\psi^b(x) + \alpha\sum_x \epsilon_{abcd}\psi^a(x)\psi^b(x)\psi^c(x)\psi^d(x) + \beta\sum_{x,\mu,\pm} \epsilon_{abcd}\psi^a(x)\psi^b(x)\psi^c(x)\psi^d(x\pm\mu) + \frac{r^2}{2}\sum_{x,\mu,\pm} \epsilon_{abcd}\psi^a(x)\psi^b(x\pm\mu)\psi^c(x)\psi^d(x\pm\mu) + \frac{r^2}{2}\sum_{x,\mu} \epsilon_{abcd}\psi^a(x)\psi^b(x\pm\mu)\psi^c(x)\psi^d(x\mp\mu) \quad (3.23)$$

where  $\alpha = \frac{G^2}{4} - rGD - \frac{2Dr^2}{4}$  and  $\beta = rG - 2r^2$ . Since we have evidence for continuous transition in  $(\kappa, G)$  plane we can keep  $r$  large enough and tune  $G$  such that we gap out all the doubler modes leaving behind a single massless

fermion. We expect that for strong coupling expansion in  $\frac{1}{r}$  with  $G \ll r$  one can analytically show that fermion propagator has the right pole structure and in the continuum limit we recover only a single massless fermion.

# Chapter 4

## Topology defects from four-fermion interactions

### 4.1 Introduction

In this chapter we construct a continuum theory of strongly interacting fermions in four dimensions in which exact symmetries prohibit the appearance of mass terms. We argue that the fermions nevertheless acquire masses at strong coupling by virtue of their interactions with a non-trivial vacuum corresponding to a symmetric four fermion condensate. Our work points out the existence of new classes of theories of strongly interacting fermions which may be important in the search for candidate theories of BSM physics.

Furthermore, we show that the theory when discretized yields a staggered fermion lattice theory which has been the focus of several recent studies both in the particle physics and condensed matter communities [1–6, 8] in both three and four dimensions. The numerical work in three dimensions is consistent with the absence of symmetry breaking bilinear condensates for all values of the four fermi coupling. The model nevertheless has a two phase structure

with a continuous phase transition with non-Heisenberg exponents separating a massless phase from a phase with a symmetric four fermion condensate and massive fermions. Progress in understanding the nature of this phase diagram was given recently in [23]. In four dimensions it appears that a very narrow symmetry broken phase emerges between the massless and massive phases.

The ingredients of the theory are somewhat unusual; the fermions appear as components of a (reduced) Kähler-Dirac field and as a consequence the theory is invariant only under a diagonal subgroup of the Lorentz and flavor symmetries together with an additional  $SO(4)$  symmetry. It is this reduced symmetry, which is enforced by the structure of the four fermion term, that plays a key role in prohibiting conventional Dirac mass terms.

Our work offers a way to understand the structure of the four dimensional models from a continuum perspective where we will see that that topological features of the continuum theory can play an important role.

## 4.2 Four fermion theory

To start consider a theory comprising 4 flavors of free massless Dirac fermion with (Euclidean) action

$$S = \int d^4x \bar{\psi}^a \gamma_\mu \partial_\mu \psi^a(x) \quad (4.1)$$

This is invariant under the global symmetry  $SO_{\text{Lorentz}}(4) \times SU_{\text{flavor}}(4)$ . To build the model of interest let us focus on the diagonal subgroup of the Lorentz symmetry and an  $SO(4)$  subgroup of the original  $SU(4)$  flavor symmetry which we call  $\mathcal{T}$ .

$$\mathcal{T} = SO'(4) = \text{diag} [SO_{\text{Lorentz}}(4) \times SO_{\text{flavor}}(4)] \quad (4.2)$$

Under this symmetry we may rewrite the action as

$$S = \int d^4x \operatorname{Tr} (\bar{\Psi} \gamma_\mu \partial_\mu \Psi) \quad (4.3)$$

where we now treat the fermions as  $4 \times 4$  matrices and the trace operation  $\operatorname{Tr}$  occurring here and throughout the chapter acts only on the matrix indices associated with the  $\mathcal{T}$  symmetry. Actually, since the theory is massless we can decompose these matrices into two independent components using the twisted chiral projectors:

$$\Psi_\pm = \frac{1}{2} (\Psi \pm \gamma_5 \Psi \gamma_5) \quad (4.4)$$

and the fermion action can be reduced to two Dirac flavors with action

$$S = \int d^4x \operatorname{Tr} (\bar{\Psi}_+ \gamma_\mu \partial_\mu \Psi_-) \quad (4.5)$$

Notice that this projection only commutes with the  $SO(4)$  subgroup of the original  $SU(4)$  flavor symmetry. In the appendix we show that this reduction is equivalent to imposing the reality condition  $\bar{\Psi} = \Psi$  with action

$$S = \int d^4x \operatorname{Tr} (\Psi \gamma_\mu \partial_\mu \Psi) \quad (4.6)$$

The equation of motion that follows from this action can be interpreted as the (reduced) Kähler-Dirac equation if one expands the fermion matrices on products of Dirac gamma matrices [24]. For the model we want to discuss we will consider four copies of this system by taking these matrix fermions to additionally transform in the fundamental representation of an independent  $SO(4)$  symmetry  $\mathcal{S}$  i.e  $\Psi^\alpha \rightarrow R^{\alpha\beta} \Psi^\beta$  with  $R$  an element of  $SO(4)$ .

Up to this point everything we have done merely corresponds to a change of variables that serves to highlight a particular subgroup of the global symmetries - the diagonal subgroup of the Lorentz and flavor symmetries. The field content

of the model still corresponds to 8 flavors of massless Dirac fermions. However this situation changes when I add four fermion interactions of the following form

$$\delta S = \frac{G^2}{4} \int d^4x \epsilon_{\alpha\beta\gamma\delta} \text{Tr} (\Psi^\alpha \Psi^\beta) \text{Tr} (\Psi^\gamma \Psi^\delta) \quad (4.7)$$

This interaction locks the Lorentz and flavor symmetries together and ensures that the global symmetries  $\mathcal{G}$  of the theory are

$$\mathcal{G} = \mathcal{T} \times \mathcal{S} = SO'(4) \times SO(4) \quad (4.8)$$

It is of crucial importance to notice that the resultant theory does *not* admit any bilinear mass terms since  $\text{Tr} \Psi^\alpha \Psi^\alpha = 0$  and any terms of the form  $\text{Tr} \Psi^\alpha \Psi^\beta$  break the symmetry  $\mathcal{S}$ .

### 4.3 Aside: connection to (reduced) staggered fermions

The motivation for this work derives in part from recent numerical investigations of lattice models involving four reduced staggered fermions interacting through the corresponding unique four fermion interaction. In this section we will show that the continuum model described earlier when discretized naturally leads to those lattice models. One way to discretize the continuum theory is to expand the fermion matrices on position dependent products of Dirac gamma matrices [9]. Consider the original  $\Psi$

$$\Psi(x) = \sum_b \gamma^{x+b} \chi(x+b) \quad (4.9)$$

where the components of the vector  $b^i = 0, 1$  label points in the unit hypercube attached to site  $x$  in a four dimensional hypercubic lattice and

$$\gamma^b = \prod_i (\gamma_i)^{b_i} \quad (4.10)$$

Plugging this expansion into eqn.(6) and doing the trace over the gamma matrices yields the free reduced staggered fermion action comprising one single component lattice fermion at each lattice site:

$$\sum_{x,\mu} \chi(x) \eta_\mu(x) \Delta_\mu \chi(x) \quad (4.11)$$

with  $\Delta_\mu$  the symmetric difference operator and  $\eta_\mu(x) = (-1)^{\sum_{i=0}^{\mu-1} x_i}$  the usual staggered fermion phase [25, 26]. Equipping each of these fields with an index under the S symmetry and adding the four fermion terms one arrives at

$$S_{\text{stag}} = \sum_{x,\mu} \chi^a(x) \eta_\mu(x) \Delta_\mu \chi^a(x) + \frac{G^2}{4} \sum_x \epsilon_{abcd} \chi^a \chi^b \chi^c \chi^d \quad (4.12)$$

which is precisely the action studied in [3, 6]. Thus we expect that the continuum arguments described in this chapter can be applied to understand the numerical results reported for this staggered fermion system.

## 4.4 Auxiliary field action

As usual our subsequent analysis requires replacing the four fermion term given in eqn.(7) by a Yukawa coupling to an auxiliary scalar field

$$S_0 = \int d^4x \left[ iG \phi_+^{\alpha\beta}(x) \text{Tr} (\Psi^\alpha \Psi^\beta) + \frac{1}{4} (\phi_+^{\alpha\beta})^2 \right] \quad (4.13)$$



The auxiliary field is a antisymmetric matrix and satisfies a self-dual condition  $\phi_+ = \mathcal{P}^+ \phi$  where the projector  $\mathcal{P}_+$  is defined as

$$\mathcal{P}_{\alpha\beta\gamma\delta}^+ = \frac{1}{2} \left( \delta_{\alpha\gamma} \delta_{\beta\delta} + \frac{1}{2} \epsilon_{\alpha\beta\gamma\delta} \right) \quad (4.14)$$

Notice that the original four fermion interaction can be written as

$$[\text{Tr } \Psi^\alpha \Psi^\beta]_+^2 = \frac{1}{4G^2} \left( \phi_+^{\alpha\beta} \right)^2 \quad (4.15)$$

This structure ensures that  $\phi_+$  transforms in the adjoint representation under a  $SU_+(2)$  subgroup of the  $\mathcal{S}$  symmetry  $SO(4) = SU_+(2) \times SU_-(2)$ . It is a singlet under both  $SU_-(2)$  and the internal  $\mathcal{T}$  symmetries (see the appendix for more details). Furthermore, it is easy to see that the eigenvalues of the resultant fermion operator come in complex conjugate pairs. In addition each eigenvalue is doubly degenerate since the fermion operator also commutes with  $SU_-(2)$ . These facts ensure that the Pfaffian that results from integration over the fermions is in fact real, positive definite.

## 4.5 Effective Action

Returning to eqn. 4.13 we now integrate out the fermions using positivity of the Pfaffian and consider the form of the one loop effective action.

$$S_{\text{eff}} = -\frac{1}{4} \text{Tr} \ln \left( -\square + G^2 \mu^2 + G \gamma_\mu \partial_\mu \phi_+ \right) \quad (4.16)$$

where  $\phi_+^2 = \mu^2 I$  and we have absorbed the explicit factor of  $i$  into the auxiliary field to render  $\phi_+$  hermitian. Let us first consider the Coleman-Weinberg

effective potential obtained by assuming a constant auxiliary field

$$V_{\text{eff}}(\mu) = -\frac{1}{4}\text{Tr} \ln \left( \frac{-\square + G^2\mu^2}{-\square} \right) + \mu^2 \quad (4.17)$$

where we have subtracted off the value of  $V_{\text{eff}}$  at  $G = 0$  and added in the classical action for  $\phi_+$ . If we expand the remainder in powers of  $G$  it should be clear that  $V_{\text{eff}}$  develops a minimum away from the origin for sufficiently large  $G > G_c$ . Thus naively one expects the system to enter a symmetry broken state for some value of the four fermi coupling. This is the usual NJL scenario and in this case will correspond to a breaking pattern  $SU_+(2) \rightarrow U(1)$  corresponding to a vacuum manifold with the topology of  $S^2$ .

Of course to understand the dynamics of the theory in more detail we need to compute the leading terms in the effective action for  $\phi_+$  for *non constant* fields. Expanding the latter on a suitable  $4 \times 4$  basis  $T$  (see the appendix for more details) we find

$$\phi_+(x) = \sum_{a=1}^3 \phi_+^a(x) T_a = \sum_{a=1}^3 n^a(x) \sigma^a \otimes I \quad (4.18)$$

In this basis the fermion operator has a trivial dependence on  $SU_-(2)$  and we will suppress it in our subsequent analysis. For  $G > G_c$  the field  $n^a(x)$  obeys the  $O(3)$  constraint  $n^a n^a = 1$ . The effective action governing the fluctuations in  $n^a(x)$  is now given by a derivative expansion of

$$-\frac{1}{4}\text{Tr} \ln \left( I + m \frac{\gamma_\mu \partial_\mu n^a \sigma^a}{-\square + m^2} \right) \quad (4.19)$$

where  $m = G\mu$ . At leading order one encounters an  $O(3)$  symmetric term quadratic in the derivatives of  $n^a(x)$  (see the appendix)

$$a(G) \int d^4x (\partial_\mu n^a)^2 \quad (4.20)$$

However at higher orders in  $1/m$  one also encounters an additional quartic term which can play an important role in understanding the possible phases of the theory.

$$b(G) \int d^4x (\epsilon^{abc} \partial_\mu n^a \partial_\nu n^b)^2 \quad (4.21)$$

The combination of these two terms defines the Fadeev-Skyrme model which is known to possess topologically stable field configurations which we will argue can play a role in the current theory.

The analysis of the dynamics is facilitated by a further change of variables in which the  $O(3)$  vector  $n^a$  is replaced by a  $SU(2)$  matrix field which rotates  $n^a \sigma^a$  to a fixed matrix - say  $\sigma_3$ .

$$n^a(x) \sigma^a = U^\dagger(x) \sigma_3 U(x) \quad (4.22)$$

This has the immediate advantage that the nonlinear constraint  $n^a n^a = 1$  is simply replaced by the unitarity property of  $U = e^{i\theta^a \sigma^a}$  with the angular variables  $\theta$ 's unconstrained. Of course this mapping cannot be the whole story since the manifold of  $SU(2)$  is  $S^3$  not  $S^2$  and indeed it is easy to see that  $n^a$  is invariant under *local* left multiplication of  $U(x)$  by an element of  $U(1)$ :

$$U(x) \rightarrow e^{i\sigma_3 \beta(x)} U(x) \quad (4.23)$$

The action is also manifestly invariant under right multiplication by a *global*  $SU(2)$  rotation  $U \rightarrow UG$ . Thus the final effective action for  $U$  should respect both this global  $SU(2)$  symmetry and the local  $U(1)$  gauge symmetry. We can make the local invariance explicit if we replace ordinary derivatives by covariant derivatives with the leading term now being

$$S_{\text{eff}} = a(G) \int d^4x \text{tr} \left[ (D_\mu U)^\dagger (D_\mu U) \right] + \dots \quad (4.24)$$

where  $D_\mu = \partial_\mu + iA_\mu\sigma_3$  and  $A_\mu$  is an abelian gauge field needed to enforce the  $U(1)$  symmetry given in eqn. 4.23. This action is classically equivalent to the original one. However in this case one would also expect to find a Maxwell term corresponding to this exact local  $U(1)$  invariance

$$\delta S_{\text{eff}} = b(G) \int d^4x F_{\mu\nu}F_{\mu\nu} \quad (4.25)$$

Indeed, classically, the field strength can be expressed in terms of  $O(3)$  vector  $n$  [27] as

$$F_{\mu\nu} = n \cdot (\partial_\mu n \times \partial_\nu n) \quad (4.26)$$

and we see that the Maxwell term just represents the higher order term in eqn. 4.21.

In this picture a conventional broken phase for the sigma model eg  $n^a = \delta^{a3}$  leads to  $U = I$  up to gauge transformations and corresponds to a Higgs phase with photon mass  $\sqrt{a(G)}$ . Close to  $G_c$  the photon mass is large and the gauge field decouples from long distance physics so that this regime is governed by the usual  $O(3)$  sigma model action.

## 4.6 Topological defects

While the uniform phase is always a possible vacuum solution additional possibilities arise at strong coupling where the quartic term plays a role. Let us search for non-trivial field configurations. To try to keep the action finite forces us to look for solutions where  $D_\mu U \rightarrow 0$  as  $r \rightarrow \infty$  and corresponding to vanishing photon mass. This implies

$$\partial_\mu U = -iA_\mu\sigma_3 U \quad (4.27)$$

or

$$A_\mu = \frac{i}{2} \text{tr} (\partial_\mu U U^\dagger \sigma_3) \quad (4.28)$$

The long distance contribution to the action of such a configuration is then determined by the Maxwell term

$$b(G) \int d^4x \frac{1}{4} (\text{tr} \partial_\mu U \partial_\nu U^\dagger \sigma_3)^2 \quad (4.29)$$

A topological defect must then correspond to a  $U(x)$  configuration that maps non-trivially at infinity into the  $S^2$  target space. Such a mapping exists, is termed the Hopf map, and corresponds to  $\Pi_3(S^2) = \mathbb{Z}$ . If we parametrize a general  $U$  matrix as

$$U = \begin{pmatrix} \alpha_1 + i\alpha_2 & -\alpha_3 + i\alpha_4 \\ \alpha_3 + i\alpha_4 & \alpha_1 - i\alpha_2 \end{pmatrix} \quad (4.30)$$

with  $\sum_i \alpha_i^2 = 1$  then the simplest topological defect corresponds to setting  $\alpha_i = \frac{x_i}{r}$  where  $x_i$  are the four dimensional coordinates. This parametrization yields a  $S^3 \rightarrow S^3$  map but this is reduced to the Hopf map when  $U$  fields which are gauge equivalent are identified. A similar topological defect solution was constructed in a four dimensional Yang-Mills-Higgs system in [28]. The  $\alpha_i$  correspond to trigonometric functions of angles in four dimensional polar coordinates and it can easily be seen that the action given in eqn. 4.29 corresponding to such a defect diverges logarithmically with system size<sup>1</sup>. Furthermore the topological charge of this object can be obtained from the theta term corresponding to the  $U(1)$  field.

$$\frac{1}{32\pi^2} \int d^4x \epsilon_{\mu\nu\rho\lambda} \text{tr} (\partial_\mu U \partial_\nu U^\dagger \sigma_3) \text{tr} (\partial_\rho U \partial_\lambda U^\dagger \sigma_3) \quad (4.31)$$

---

<sup>1</sup>For a Hopf defect the gauge field corresponds to a large gauge transformation

Unlike the action this term does not diverge logarithmically since it may be recast as a Chern-Simons term which can be computed on the boundary sphere at infinity.

While such a background corresponds asymptotically to a point on the vacuum manifold it clearly does not break the  $\mathcal{S}$  symmetry since  $\langle \sum_x \phi_+(x) \rangle = 0$ . Of course the key question is whether such defects can play a role in determining the phase structure of the model. At first glance they should not - the logarithmically divergent action corresponding to such defects will ensure that a single defect is completely suppressed in the infinite volume limit. This situation is analogous to the behavior of vortices in the two dimensional XY model which also possess a log divergent action. In the latter case a configuration of finite action can be constructed consisting of a vortex and anti-vortex. The action for such a configuration depends logarithmically on the separation of the two vortices which hence bind tightly together at low temperatures. However since the entropy associated with a vortex also increases logarithmically with system size a BKT phase transition develops as the temperature is raised and vortices unbind and populate the ground state.

We propose that a similar phenomena may occur in this four dimensional model - that is the ground state for  $G \sim G_c$  consists of tightly bound Hopf-antiHopf defects. In such a scenario the disordering effects of the defects are suppressed and one expects a conventional symmetry broken (Higgs) phase to appear as has been observed in the numerical simulations [6, 8]. However as the coupling is increased still further the defects may unbind via another transition to populate and disorder the ground state. This condensate of Hopf defects with  $\langle \phi_+^2 \rangle \neq 0$  would then correspond to the four fermion condensate in the original four fermi model consistent with eqn. 4.15. An estimate for the critical coupling can be arrived at by comparing the entropy associated to the location of a single defect  $S \sim \ln V$  with its action  $E \sim b(G) \ln V$  yielding  $b(G)^{\text{crit}} \sim 1$ .

It is interesting to compute the fermion propagator in the background of such a defect. Consider the  $\mathcal{S}$ -symmetric correlator

$$\begin{aligned} G_F(x, y) &= \text{tr} \langle \Psi(x) \Psi(y) \rangle \\ &= \text{tr} \left[ \frac{-\gamma_\mu \partial_\mu + m n^a \sigma^a}{(-\partial_\mu^2 + m^2 + mP)} \right] \end{aligned} \quad (4.32)$$

where

$$P = \gamma_\mu (\partial_\mu U^\dagger(x) \sigma_3 U(x) + U^\dagger(x) \sigma_3 \partial_\mu U(x)) \quad (4.33)$$

and the trace is to be carried out over the  $\mathcal{S}$ -indices. Using the fact that the covariant derivative vanishes far from the core of the defect allows us to show that  $P = 0$  and the propagator in that region simplifies to

$$G_F(x, y) = \frac{-2\gamma_\mu \partial_\mu}{-\square + m^2} \quad (4.34)$$

Thus the fermion acquires a mass  $m = \mu G$  in the background of such a defect. This gives a concrete realization of the mechanism discussed in [29] and is consistent with strong coupling expansions for staggered fermions [3].

## 4.7 BKT transition

We have argued that the model possesses a conventional broken phase (or Higgs phase) which gives way to a symmetric phase at stronger coupling due to unbinding of topological defects. Since mechanisms for giving fermions a mass are quite different in the two regimes one might expect a discontinuous phase transition separates the broken phase and the defect phase. To obtain a true BKT-like transition requires one to pass directly between the massless and massive symmetric phases. To effect such a scenario one can generalize the original four fermion model to a true Higgs-Yukawa model by the addition of a kinetic

term for the auxiliary field  $\phi_+$ . One can then imagine tuning the coupling of this kinetic operator so as to cancel out the effects of the leading gradient term eqn. 4.24. This sets the photon mass to zero and eliminates the Higgs phase of the model. We conjecture that in this limit a true single BKT transition separates the massless and massive phases.

## 4.8 Summary

We have argued that a particular four dimensional continuum theory possesses an interesting phase structure as a function of the coupling to a particular four fermion interaction. For sufficiently weak four fermi coupling we expect the theory to describe massless non-interacting fermions. As the coupling is increased the system should undergo a NJL-like phase transition to a phase in which the  $SO(4)$  symmetry is spontaneously broken via a bilinear fermion condensate. In the auxiliary field picture this phase is characterized by tightly bound pairs of Hopf defects and a non-zero expectation value for the scalar field. As the coupling is increased further we argue that these defects may unbind at a transition to populate and disorder the vacuum restoring the symmetry. In the background of such defects the fermions acquire a mass without breaking symmetries. This phase is interpreted as a four fermion condensate in the original fields. We also argue that by an additional tuning of the kinetic energy the broken phase can be eliminated and a single BKT transition would separate the massless from massive phases.

The continuum theory we describe possesses an unusual Lorentz symmetry which is locked via the four fermion interaction with an internal flavor symmetry. At weak coupling we expect the four fermi term to be irrelevant and the IR description of the theory will correspond to sixteen flavors of free Majorana fermion with the symmetry enhancing to the usual Lorentz and flavor symme-



tries. Correspondingly the beta function for the four fermi coupling has an IR attractive fixed point at  $G = 0$ . The transition to a phase of broken symmetry is likely of the NJL type and hence the corresponding (IR unstable) fixed point would lie in the universality class of the usual Higgs-Yukawa theory. However if an additional continuous transition were to separate this phase from the four fermion condensate phase this would correspond to a new strongly coupled IR fixed point. This would be a fascinating prospect. The BKT limit would correspond to a situation where the two fixed fixed points bounding the broken phase merge into a single continuous transition.

We have also argued that this continuum theory naturally discretizes to yield a theory of strongly interacting reduced staggered fermions. This lattice model has received some recent attention and the numerical phase diagram that has been uncovered matches quite closely with the gross features described in this chapter. Indeed, in the condensed matter literature there has recently been a great deal of interest in models which are able to gap fermions without breaking symmetries using carefully chosen quartic interactions [11]. This work has even been used to revive an old approach to lattice chiral gauge theories due to Eichten and Preskill [30] in which mirror states of a definite chirality can be gapped out of an underlying vector like lattice theory using four fermion interactions [31]. It will be interesting to see whether the current model can be generalized to implement such constructions. Independent of this potential connection, the possibility of new phases and critical points in strongly interacting fermion systems in four dimensions is very interesting in its own right and we hope the current work stimulates further work in this area.

## 4.9 Appendix

### Obtaining the twisted Majorana form

Setting  $\bar{\Psi}_+ = C^{-1}\Psi_+^T C$  where  $C$  is the charge conjugation operator the action can be rewritten

$$S = \int d^4x \text{Tr} (C^{-1}\Psi_+^T C \gamma_\mu \partial_\mu \Psi_-) \quad (4.35)$$

Taking the transpose of this equation yields

$$S = \int d^4x \text{Tr} (C^{-1}\Psi_-^T C \gamma_\mu \partial_\mu \Psi_+) \quad (4.36)$$

Adding these two expressions the action can be expressed entirely in terms of the field  $\Psi = \Psi_+ + \Psi_-$ .

$$S = \int d^4x \text{Tr} (C^{-1}\Psi^T C \gamma_\mu \partial_\mu \Psi) \quad (4.37)$$

But  $C^{-1}\Psi^T C = \Psi$  if one expresses the matrix  $\Psi$  as a sum over the Clifford algebra formed from the product of Dirac gamma matrices so that the action in (twisted) Majorana form is simply

$$S = \int d^4x \text{Tr} (\Psi \gamma_\mu \partial_\mu \Psi) \quad (4.38)$$

### Changing basis to $SU(2) \times SU(2)$

We can verify the mapping into the  $O(3)$  non-linear sigma model by starting from an explicit  $4 \times 4$  basis for the hermitian self-dual field  $\phi_+ = \sum_{a=1}^3 \phi_+^a T_a$

$$T_1 = \begin{pmatrix} 0 & -i\sigma_1 \\ i\sigma_1 & 0 \end{pmatrix} \quad T_2 = \begin{pmatrix} 0 & i\sigma_3 \\ -i\sigma_3 & 0 \end{pmatrix} \quad T_3 = \begin{pmatrix} \sigma_2 & 0 \\ 0 & \sigma_2 \end{pmatrix}$$

These matrices clearly obey an  $SU(2)$  algebra which is part of the original  $SO(4)$   $\mathcal{S}$  algebra and the self-dual condition is clearly equivalent to the statement that  $\phi_+$  transforms in the adjoint representation of that  $SU(2)$ . The other independent  $SU(2)$  contained in  $\mathcal{S}$  is given the generators

$$U_1 = \begin{pmatrix} 0 & -\sigma_2 \\ -\sigma_2 & 0 \end{pmatrix} \quad U_2 = \begin{pmatrix} 0 & i\sigma_1 \\ -i\sigma_1 & 0 \end{pmatrix} \quad U_3 = \begin{pmatrix} \sigma_2 & 0 \\ 0 & -\sigma_2 \end{pmatrix}$$

Using the similarity transformation  $P$  given by

$$P = \frac{1}{\sqrt{2}} \begin{pmatrix} 1 & 0 & 0 & -1 \\ i & 0 & 0 & i \\ 0 & -1 & -1 & 0 \\ 0 & -i & i & 0 \end{pmatrix} \quad (4.39)$$

one can verify that the generators  $T$  and  $U$  take the form

$$T^a = \sigma^a \otimes I \quad \text{and} \quad U^a = I \otimes \sigma^a \quad (4.40)$$

This makes it clear that  $T^a$  (and hence  $\phi_+$ ) are singlets under  $SU_-(2)$ .

## Coleman-Weinberg potential

The path integral over the Kahler-Dirac fermions yield the Pfaffian

$$\int d\Psi d\phi_+ e^{-\int d^4x [\text{Tr}(\Psi \gamma^\mu \partial_\mu \Psi) + iG\phi_+^{\alpha\beta} \text{Tr}(\Psi^\alpha \Psi^\beta) + \frac{1}{4}(\phi_+^{\alpha\beta})^2]} \quad (4.41)$$

$$Pf[\gamma^\mu \partial_\mu + G\phi_+] = \exp\left[\frac{1}{2} \text{Tr} \ln(\gamma^\mu \partial_\mu + G\phi_+)\right] \quad (4.42)$$

Since we are interested in the effective potential we can treat  $\phi = \mu$  as a constant over space-time. In four dimensions

$$\text{Tr} \ln(\gamma^\mu \partial_\mu + m) = \int \frac{d^4x d^4p}{(2\pi)^4} \ln(p^2 + m^2) \quad (4.43)$$

where  $m = \mu G$ . The effective potential is

$$V_{eff}(\mu^2) = \frac{1}{4} \mu^2 G^2 + \frac{\mu^4 G^4}{2(4\pi)^2} \left( \ln\left(\frac{\mu^2 G^2}{\Lambda^2}\right) + \frac{3}{2} \right) \quad (4.44)$$

where  $\Lambda$  is momentum cut-off. The minimum of the potential with respect to  $\mu$  varies as  $G$  changes with a fixed  $\Lambda$ . When  $G \gg \Lambda$  the only minimum of the effective potential occurs for  $\mu = 0$  which implies that there is no symmetry breaking in the system. For  $G$  comparable to  $\Lambda$  the potential develops unstable minimas close to the true minimum  $\mu = 0$ .

## Bosonic propagator

If the effective potential develops a minimum away from the origin then we can assume that there is symmetry breaking in the system. Hence in the broken phase can assume that  $\phi = \mu$ . In this limit we can compute the two-point function using standard perturbation theory

$$\Gamma(p^2) = \int \frac{d^4k}{(2\pi)^4} \text{tr} \left[ \frac{1}{\gamma^\mu k_\mu + m} \frac{1}{\gamma^\mu (k_\mu + p_\mu) + m} \right] \quad (4.45)$$

The total two-point function is

$$\Gamma(p^2) = -\alpha - \frac{1}{2\pi} \int_0^1 dx \ln \frac{-x(1-x)p^2 + m^2}{m^2} \quad (4.46)$$

An important thing to notice here is that at lowest order in  $p^2$

$$\Gamma(p^2) = \frac{1}{2\pi} \int_0^1 dx x(1-x) \frac{p^2}{m^2} = \frac{1}{2\pi} \frac{p^2}{m^2} \quad (4.47)$$

In real space this term corresponds to

$$\int d^4x \frac{1}{2\pi} \frac{1}{m^2} (\partial_\mu n^a)^2 \quad (4.48)$$

### Large $m$ expansion

The effective action is generated by integrating fermions which results in the determinant of fermion operator which is

$$D = \gamma^\mu \partial_\mu + mn^a \sigma^a \quad (4.49)$$

The effective action

$$S_{eff} = -\frac{1}{8} \text{Tr} \ln(-\square + m^2 + m\gamma^\mu \partial_\mu n^a \sigma^a) \quad (4.50)$$

Defining  $G_o = (-\square + m^2)^{-1}$

We can write the effective action as

$$S_{eff} = -\frac{1}{8} \text{Tr} \ln(1 + G_o m \gamma^\mu \partial_\mu n^a \sigma^a) \quad (4.51)$$

Expanding in  $1/m$  we have

$$S_{eff} = -\frac{1}{8} \text{Tr} \sum_{k \geq 0} \frac{(-1)^k (\gamma^\mu \partial_\mu n^a \sigma^a)^{k+1}}{(k+1)m^{k+1}} \quad (4.52)$$

where the  $\text{Tr}$  denotes trace over internal indices and a functional trace. The functional traces can be easily computed by going to momentum space. We use

$\text{Tr}(\hat{X}) = \int d^4x \langle x | \hat{X} | x \rangle$  for functional traces. The first non-vanishing term is at  $k = 1$

$$S_{eff}^{(1)} = \int d^4x \frac{\Lambda^4}{2m^2} (\partial_\mu n^a)^2 \quad (4.53)$$

where  $\Lambda$  is the UV(IR) cut-off in the theory. It's essential to render the effective dimensionless. The next interesting term emerges for  $k = 3$

$$S_{eff}^{(3)} = \frac{1}{4m^4} \text{Tr}(\gamma^\mu \gamma^\nu \gamma^\rho \gamma^\sigma) \text{tr}(\epsilon^{abe} \partial_\mu n^a \partial_\nu n^b \epsilon^{cde} \partial_\rho n^c \partial_\sigma n^d) \quad (4.54)$$

where  $\text{tr}$  implies a functional trace. We have used the standard relation  $\sigma^a \sigma^b = \delta^{ab} + i\epsilon^{abc} \sigma^c$  in simplifying the expression. Defining  $F_{\mu\nu}^e = \epsilon^{abe} \partial_\mu n^a \partial_\nu n^b$  and going to momentum space one can compute the final expression after a little bit of algebra. Moreover the definition  $F_{\mu\nu} = \epsilon^{abc} n^a \partial_\mu n^b \partial_\nu n^c$  in the literature is more useful in the background of topological current. Here this Maxwell type term naturally arises from the derivative expansion. Putting it all together the effective action takes the form

$$S_{eff} = \frac{1}{2} \int d^4x \frac{\Lambda^4}{m^2} (\partial_\mu n^a)^2 + \int d^4x \frac{\Lambda^4}{m^4} (F_{\mu\nu})^2 \quad (4.55)$$

The pre-factors for the quadratic term and quartic term both depend on  $m$  but we will treat them as independent couplings as they will flow differently in RG analysis.

# Chapter 5

## $SU(2)$ lattice gauge theory with reduced staggered fermions

### 5.1 Introduction

Simulations of gauge theories using staggered fermions have a long history going back to the early days of lattice gauge theory. In recent years they have allowed for precision studies of hadronic quantities of crucial importance to experimental efforts to test and constrain the Standard Model [32].

As is well known the four dimensional naive staggered fermion action yields not one but four Dirac fermions in the continuum limit. It is less well appreciated that this replication can be halved by an additional thinning of lattice degrees of freedom to create what are called *reduced* staggered fermions. At first glance this fact seems to imply that the reduced fermion would be a better choice than the usual staggered fermion for simulations. It was realized early on that this was not the case; for QCD the resulting fermion determinant is not real, positive definite and furthermore it is not possible to write gauge invariant single site mass terms in such a theory [26].

In this chapter we point out that these problems can be evaded for gauge groups with pseudoreal representations. As an example we consider the case of fermions transforming in the fundamental representation of  $SU(2)$ . Quenched simulations of this model have been studied in [33] but the only work we are aware of with dynamical fermions was carried out in the context of a four fermion model with off-site Yukawa couplings [34]. In this paper we study the case of the  $SU(2)$  gauge theory with both single site and one-link mass terms. We show that the corresponding single site fermion condensate dominates at strong coupling in the thermodynamic limit as the fermion masses are sent to zero. The appearance of a single site condensate breaks the one remaining global  $U(1)$  symmetry in the reduced fermion action and leads to a light pion which is also measured in our simulations. This  $U(1)$  symmetry breaking is consistent with the RMT analysis of [35].

Consider a continuum non-abelian gauge theory with  $N$  flavors of Dirac fermion coupled vectorially. The fermions transform in an irreducible representation of the gauge group. With  $N$  flavors we have the chiral-flavor symmetry  $SU(N) \times SU(N)$ . If this symmetry spontaneously breaks the symmetry breaking pattern will depend on the nature of the color representation carried by fermions. The term which breaks the chiral symmetry is  $\bar{\Psi}\Psi$  and surviving flavor symmetry falls into three classes discussed in [35]. Previous studies used the distribution of smallest eigenvalues of Dirac operator to show spontaneous chiral symmetry breaking. This approach comes from Banks-Casher relation

$$\Sigma = \pi\rho(0) \tag{5.1}$$

which states that non-zero density of Dirac operator eigenvalues close to origin is a signal for spontaneous chiral symmetry breaking. To explore the spectral densities around the origin Random Matrix theory methods are used. However for



staggered fermions in real or pseudo-real representation the symmetry breaking pattern doesn't follow the continuum analogs and we get the wrong Goldstone spectrum. This has been long known in the lattice literature. The studies we know of used quenched approximations for spectral measurements and no full-scale dynamical Monte-Carlo simulation have been done so far. In this study we will compute the chiral condensate by numerical means on a lattice. The approach we will take is based on the definition of chiral condensate.

$$\Sigma = \lim_{m \rightarrow 0} \lim_{V \rightarrow \infty} \langle \bar{\Psi} \Psi \rangle \quad (5.2)$$

The infinite volume limit needs to be taken before the massless limit  $m \rightarrow 0$ . In order to understand how staggered fermions in pseudo-real representation have the wrong chiral symmetry breaking compared to continuum Dirac fermions let's take a look at the term which breaks the chiral symmetry and simultaneously preserves maximal flavor symmetry. The continuum term is

$$\epsilon_{\alpha\beta} \psi_{\alpha}^{ia} \psi_{\beta}^{jb} U_{ab}^{-1} V_{ij} \quad (5.3)$$

where  $\alpha, i, a$  are the spinor, flavor and color indices respectively. Since the fermions are in a pseudo-real representation the right-handed fermion  $\chi$  transforms as  $U\psi$  where  $U$  is a *antisymmetric* unitary matrix with the property  $UU^* = -1$ . The original  $SU(N) \times SU(N)$  is enlarged to  $SU(2N)$  due to the pseudo-real nature of color representation however the Grassmann nature of fermion fields forces the surviving flavor symmetry to be symplectic hence breaking  $SU(2N) \rightarrow Sp(2N)$ . Using  $N$  flavors of staggered fermions we have usual  $U_e(N) \times U_o(N)$  symmetry which is enhanced to  $U(2N)$  with pseudo-real color representation [35]. However for staggered fermions we lose the spinor indices as the fermions are single

component objects. Hence for staggered fermion  $\chi$  bilinear term is

$$\chi^{ia}\chi^{jb}U_{ab}^{-1}V_{ij} \quad (5.4)$$

If  $V = -V^T$  then this term is trivially zero. If  $V = V^T$  then this term is non-vanishing however now  $U(2N)$  breaks to  $O(2N)$ . This discussion is valid for staggered fermions but we are using *reduced* staggered fermions. An obvious question to ask here is the equivalence of *reduced* staggered and full staggered formalism. It is straightforward to see that staggered Dirac operator is anti-Hermitian with pure imaginary spectrum. The *reduced* staggered Dirac operator is anti-symmetric but not anti-Hermitian. *Reduced* staggered operator satisfies the simple property

$$(\Delta_\mu)^\dagger = -\sigma_2\Delta_\mu\sigma_2 \quad (5.5)$$

The spectrum carries complex eigenvalues paired as  $\lambda, \bar{\lambda}$  due to pseudo-real nature of the gauge group and  $\lambda, -\lambda$  due to anti-symmetry. Combining them the spectrum is  $(\lambda, -\lambda, \bar{\lambda}, -\bar{\lambda})$ . For *reduced* staggered field  $\psi$  with  $N$  flavors the bilinear term is

$$\psi^{ia}\psi^{jb}U_{ab}V_{ij} \quad (5.6)$$

where both  $U, V$  are anti-symmetric which has the same exact form as full staggered bilinear. Despite the spectral difference from full staggered case the bilinear term for *reduced* case has an  $O(2N)$  symmetry. In other words both formalisms have the same symmetry breaking pattern.

This chapter is divided into two sections. In the second section we will introduce the lattice action and discuss how the bilinear term for staggered fermions differs from continuum Dirac mass term. In the third section we will present numerical results which validates the conjectured symmetry breaking pattern. One of our motivations for this work comes from four fermion model studied

in previous two chapters. In four dimensions a very narrow broken symmetry phase reappears between the weak and strong coupling phases [3, 6] but there is evidence that this broken symmetry phase may be evaded in an expanded phase diagram corresponding to a Higgs-Yukawa generalization of the model [10, 36]. This latter model possesses a global  $SO(4) = SU(2) \times SU(2)$  symmetry with the Yukawa interaction coupling the staggered fermions to a scalar field living in the adjoint representation of one of these  $SU(2)$ s. A natural extension of this model then replaces the scalar field with an  $SU(2)$  gauge field which we conjecture is capable of generating the same four fermion condensate now via strong gauge interactions. As a first step in this direction we need to understand the phase structure and symmetry breaking patterns of reduced staggered fermions interacting via a  $SU(2)$  gauge field - the study reported here.

## 5.2 Action and symmetries

For completeness we repeat here the derivation of the reduced staggered fermion action [26]. Starting with the full *massless* staggered action

$$S_F = \sum_{x,\mu} \frac{1}{2} \eta_\mu(x) \bar{\psi}(x) [U_\mu(x) \psi(x + \mu) - U_\mu^\dagger(x - \mu) \psi(x - \mu)] \quad (5.7)$$

where the staggered fermion phases are given by

$$\eta_\mu(x) = (-1)^{\sum_{i=1}^{\mu-1} x_i} \quad (5.8)$$

we project down to *reduced* staggered variables.

$$\begin{aligned} \bar{\psi}(x) &\rightarrow \frac{1 + \epsilon(x)}{2} \bar{\psi}(x) \\ \psi(x) &\rightarrow \frac{1 - \epsilon(x)}{2} \psi(x) \end{aligned} \quad (5.9)$$

where the parity factor  $\epsilon(x) = (-1)^{\sum_{i=1}^4 x_i}$ . Since  $\bar{\psi}$  is only defined on even sites we can relabel it as  $\psi^T$ . Furthermore, we can introduce a new gauge field  $\mathcal{U}_\mu(x)$  defined by

$$\mathcal{U}_\mu(x) = \frac{1 + \epsilon(x)}{2} U_\mu(x) + \frac{1 - \epsilon(x)}{2} U_\mu^*(x) \quad (5.10)$$

and rewrite the resultant *reduced* staggered action in the form

$$S_F = \sum_{x,\mu} \frac{1}{2} \eta_\mu(x) \psi^T(x) \mathcal{U}_\mu(x) \psi(x + \mu) \quad (5.11)$$

By taking the transpose of this equation it can be written equivalently as

$$S_F = \sum_{x,\mu} \frac{1}{2} \psi^T(x) \eta_\mu(x) \Delta_\mu(x) \psi(x) \quad (5.12)$$

where

$$\Delta_\mu \psi(x) = \frac{1}{2} (\mathcal{U}_\mu(x) \psi(x + \mu) - \mathcal{U}_\mu^T(x - \mu) \psi(x - \mu)) \quad (5.13)$$

which reveals explicitly the antisymmetric character of the reduced fermion operator. This reduced action is invariant under two symmetries in addition to gauge invariance, a continuous  $U(1)$  symmetry which acts on the fermions

$$\psi(x) \rightarrow e^{i\alpha\epsilon(x)} \psi(x) \quad (5.14)$$

and discrete shift symmetry

$$\psi \rightarrow \xi_\rho \psi(x + \rho) \quad (5.15)$$

where  $\xi_\mu = (-1)^{\sum_{i=\mu+1}^{d-1} x_i}$ . Since for reduced fermions one keeps only  $\psi$  or  $\bar{\psi}$  at each site the usual staggered fermion mass term does not exist. However  $\psi^a \psi^b \epsilon_{ab}$  is clearly a gauge invariant fermion bilinear for fermions transforming in the fundamental representation of  $SU(2)$  and can hence be added to the

fermion action<sup>1</sup>.

$$\delta S = O_S = m \sum_x \epsilon(x) \psi^a(x) \psi^b(x) \epsilon_{ab} \quad (5.16)$$

To understand why the parity factor  $\epsilon(x)$  appears in the mass term consider the full fermion operator

$$D = \eta_\mu(x) \Delta_\mu^{ab} + m \epsilon(x) \epsilon^{ab} \quad (5.17)$$

The poles of the associated propagator are determined by the zeroes of  $D^2$ . Using the fact that the parity operator  $\epsilon(x)$  anticommutes with the symmetric difference operator  $\Delta_\mu$  allows one to write

$$-D^2 = -\Delta^\mu \Delta_\mu + m^2 \quad (5.18)$$

which exhibits the correct pole structure for a massive fermion (in Euclidean space). Notice that this mass operator induces the breaking  $U(1) \rightarrow Z_2$ . Alternatively, we can retain the  $U(1)$  symmetry by adding a gauge invariant one link mass term which then breaks the shift symmetry.

$$O_L = m_1 \sum_{x,\mu} \frac{1}{2} \xi_\mu(x) \epsilon(x) \psi^T(x) \mathcal{M}_\mu \psi(x) \quad (5.19)$$

where

$$\mathcal{M}_\mu \psi(x) = \frac{1}{2} [\mathcal{U}_\mu(x) \psi^b(x + \mu) + \mathcal{U}_\mu^T(x - \mu) \psi(x - \mu)] \quad (5.20)$$

Notice the addition of  $O_S$  and  $O_L$  to the action preserves the antisymmetry of the fermion operator. In our numerical work we have investigated the effects of both of these mass terms. For a full staggered field the symmetry breaking patterns are a little different. For such a staggered field in a pseudoreal

---

<sup>1</sup>Notice the analog of this term vanishes for two continuum Weyl fermions because of an additional contraction over Lorentz indices unless the fermions carry additional flavor indices.

representation we can pair the  $\psi$  and  $\bar{\psi}$  at each site into a doublet with the kinetic operator now being invariant under a  $U(2)$  symmetry. In this case a site mass term now breaks  $U(2) \rightarrow O(2)$ . Such a symmetry breaking pattern could also be obtained by using two reduced staggered fields. Once we integrate the fermions we generate a Pfaffian. Since the fermion operator is antisymmetric its eigenvalues come in pairs  $(\lambda, -\lambda)$ . Additionally the pseudo-real nature of the representation implies that  $U_\mu^*(x) = \sigma_2 U_\mu(x) \sigma_2$  which ensures that every eigenvalue  $\lambda_n$  (generically complex) and corresponding eigenvector  $v_n$  is paired with another with eigenvalue  $\lambda_n^*$  and eigenvector  $\sigma_2 v_n^*$ . This quartic structure of the spectrum ensures that the Pfaffian is positive definite and can hence be written  $Pf(D) = \det(D^\dagger D)^{\frac{1}{4}}$  which is suitable for use in a Monte Carlo algorithm [37]<sup>2</sup>. For the gauge part of the  $SU(2)$  action we employ the standard Wilson action

$$S_G = \sum_x \sum_{\mu < \nu} -\frac{\beta}{2N} \text{Tr}[U_{\mu\nu}(x) + U_{\mu\nu}^\dagger(x)] \quad (5.21)$$

The full action used for lattice simulation is given by

$$S = S_F + S_G + O_S + O_L \quad (5.22)$$

### 5.3 Numerical Results

We implemented the RHMC algorithm to simulate the model exploring lattice volumes up to  $16^4$  with gauge couplings spanning  $\beta = 0.85 - 4.0$  and for a wide range of site and link masses. Fig. 5.1 and fig. 5.2 show plots of the expectation values of the site and link bilinears for  $m = m_1 = 0.1$  as a function of the gauge coupling  $\beta$  for several lattice volumes. Both vevs are driven to small values for large  $\beta$  as expected since the model enters a deconfined phase in that

---

<sup>2</sup>An exception to this can occur if the fermion operator develops a purely real eigenvalue which is then unpaired. We have seen no sign of such eigenvalues in our simulations.

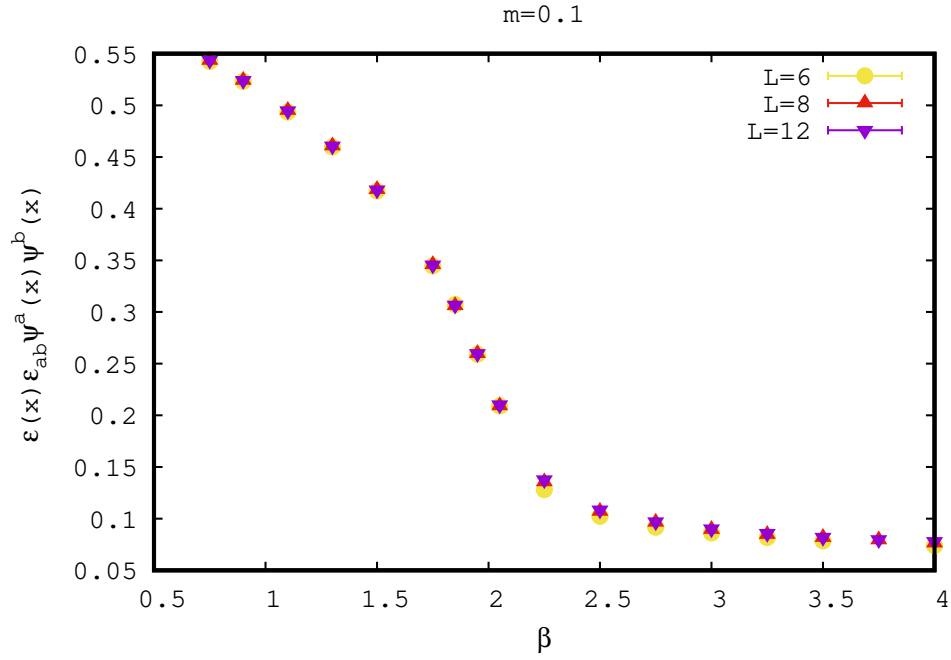


Figure 5.1:  $\langle O_S \rangle$  with  $m = m_1 = 0.1$  for  $L = 6, 8, 12$

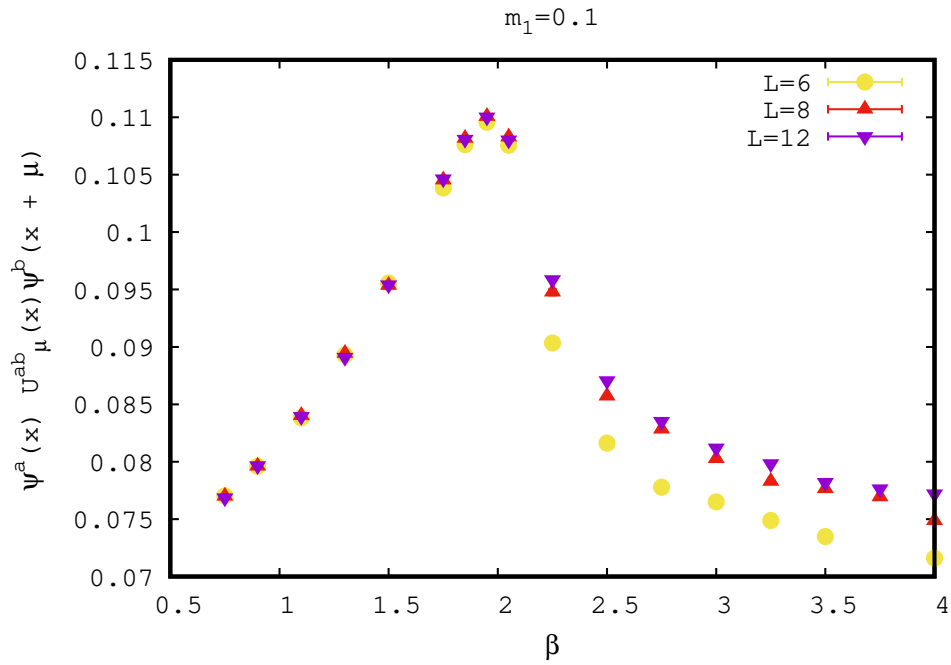


Figure 5.2:  $\langle O_L \rangle$  with  $m = m_1 = 0.1$  for  $L = 6, 8, 12$

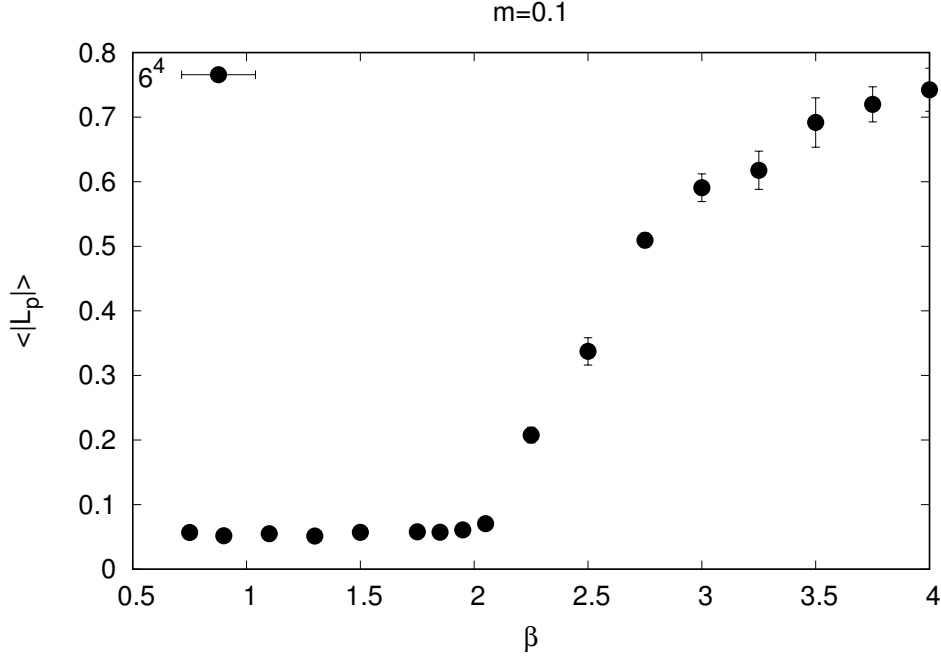


Figure 5.3:  $\langle |L_p(x)| \rangle$  Polyakov line for  $L = 6$  and  $m = 0.1$

regime which can be seen clearly in fig. 5.3 which shows the Polyakov line as a function of gauge coupling for  $m = m_1 = 0.1$  on a  $6^4$  site lattice. The Polyakov line functions as a quasi-order parameter for the breaking of center symmetry and runs from small to large values as the system deconfines. However in a dynamical setup Polyakov line susceptibility doesn't show anything interesting for characterizing the order of transition. Of course the key question is whether one or more of these bilinears vev remains nonzero in the thermodynamic limit as the bare fermion mass is sent to zero. We focus on the largest values of the (inverse) gauge coupling (smallest lattice spacing) which clearly lie within the confining regime of the theory on the lattice volumes we have simulated.

In fig. 5.4 and fig. 5.5 we show plots of the expectation values of the two bilinears versus the bare fermion mass  $m = m_1$  for gauge coupling  $\beta = 1.8$  for a range of lattice volumes. Clearly the link vev shows no strong volume dependence and smoothly goes to zero as the external mass is sent to zero.



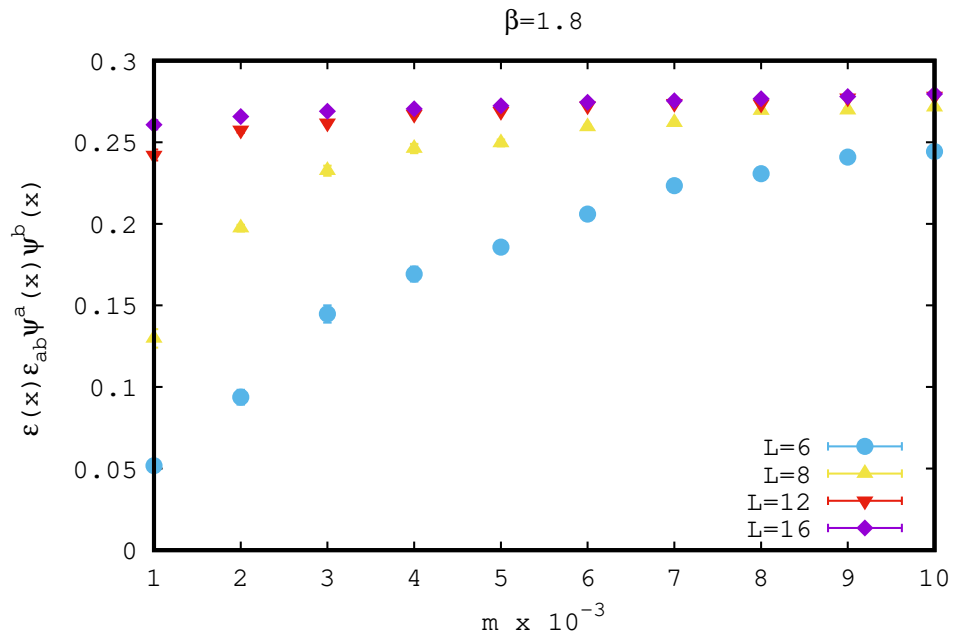


Figure 5.4:  $\langle O_S \rangle$  vs  $m$  at  $\beta = 1.8$  for  $L = 6, 8, 12, 16$

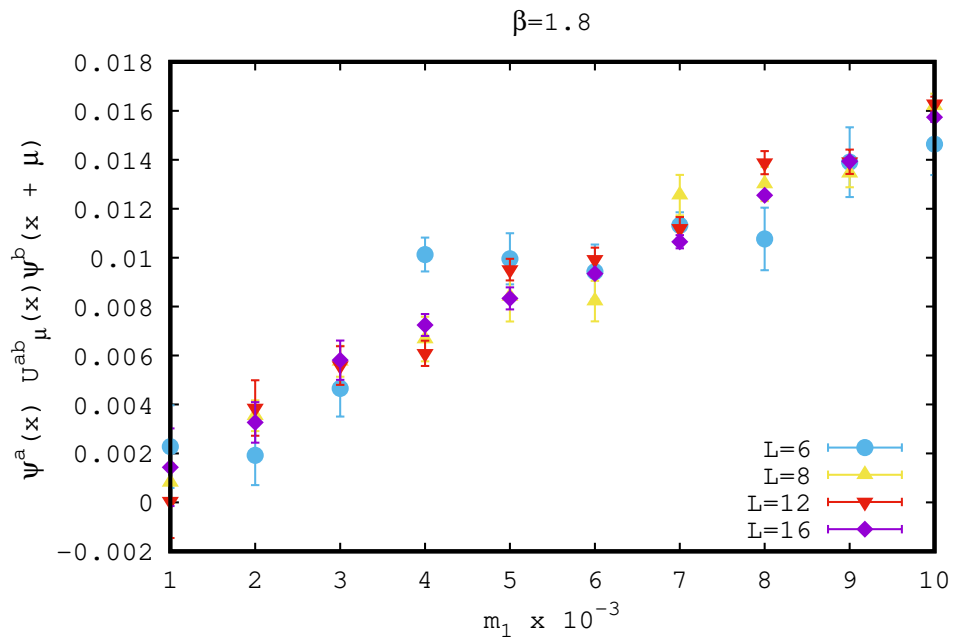


Figure 5.5:  $\langle O_L \rangle$  vs  $m_1$  at  $\beta = 1.8$  for  $L = 6, 8, 12, 16$

This is consistent with work by Follana et al [33] for full staggered fermions in quenched approximation. The site bilinear shows a very different behavior with the measured vev growing with volume at small mass. This is the behavior needed for a non-zero condensate to survive the zero mass limit and indeed the data is quite consistent with the presence of a non-zero site condensate in that limit. To gain confidence in this result we repeated the analysis for  $\beta = 1.7$  (fig. 5.6 and fig. 5.7) corresponding to a larger value of the lattice spacing. The overall conclusion remains the same and we infer that the preferred breaking channel for the simple reduced staggered fermions studied here corresponds to  $U(1) \rightarrow Z_2$ <sup>3</sup> We can confirm these conclusions by looking for the corresponding Goldstone boson - the pion - whose correlator is given by

$$\langle \phi(x)\phi(y) \rangle = \langle \epsilon^{ab}\psi^a(x)\psi^b(x)\epsilon^{cd}\psi^c(y)\psi^d(y) \rangle \quad (5.23)$$

A typical correlator is shown at  $m = 0.1$  and  $\beta = 1.8$  on a  $8^3 \times 32$  lattice in Fig. 5.8. We use the standard fit  $C_\pi(t) \sim A [\exp(-am_\pi(t)) + \exp(-am_\pi(T-t))]$  to extract the pion mass. In Fig. 5.9 we plot the pion mass as a function of the bare quark mass  $m$ . For this calculation the smallest quark mass we use is  $m = 0.01$  which ensures safe distance from epsilon regime where finite volume effects drive the condensate to zero in  $m \rightarrow 0$  limit. The solid line is a fit to the expected square root form and corresponds to the standard GMOR prediction confirming that this state is indeed a pion resulting from spontaneous breaking of the  $U(1)$  symmetry.

---

<sup>3</sup>Similar results were observed by Follana [33] in the quenched approximation although the nature of the condensate changed when a smeared action was employed.

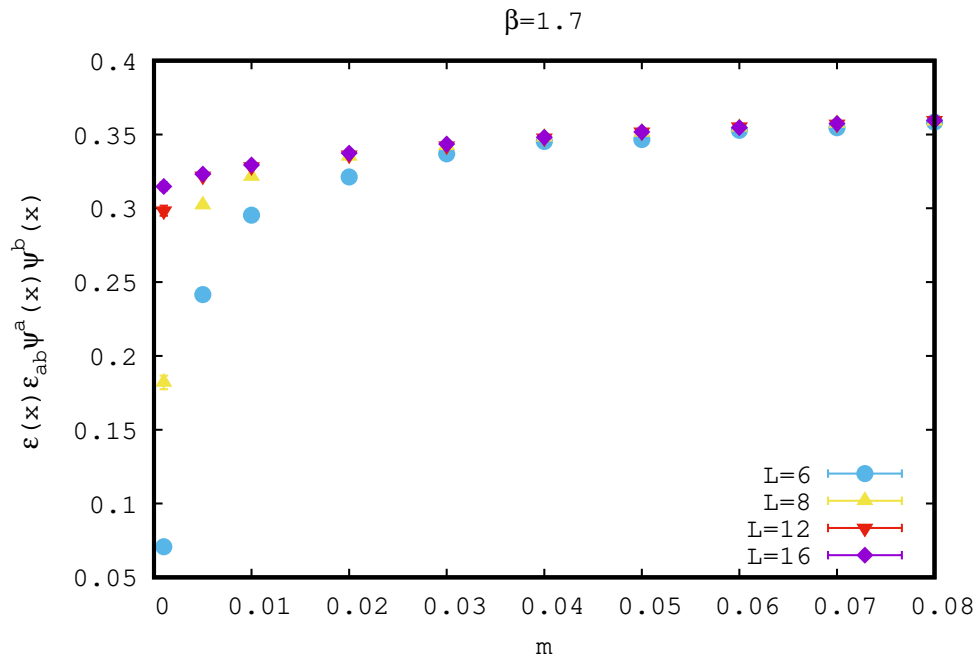


Figure 5.6:  $\langle O_S \rangle$  vs  $m$  at  $\beta = 1.7$  for  $L = 6, 8, 12, 16$

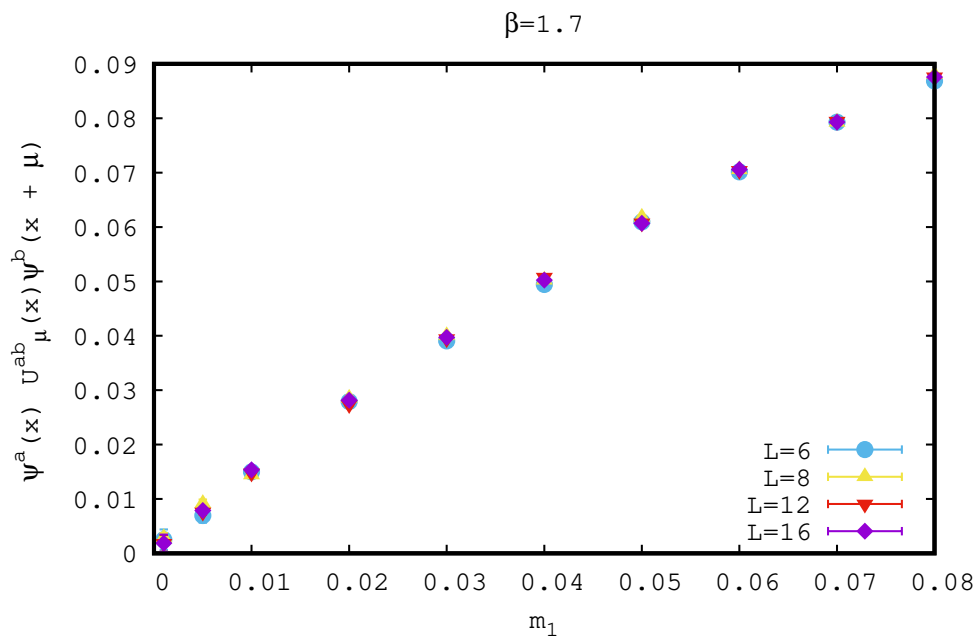


Figure 5.7:  $\langle O_L \rangle$  vs  $m_1$  at  $\beta = 1.7$  for  $L = 6, 8, 12, 16$

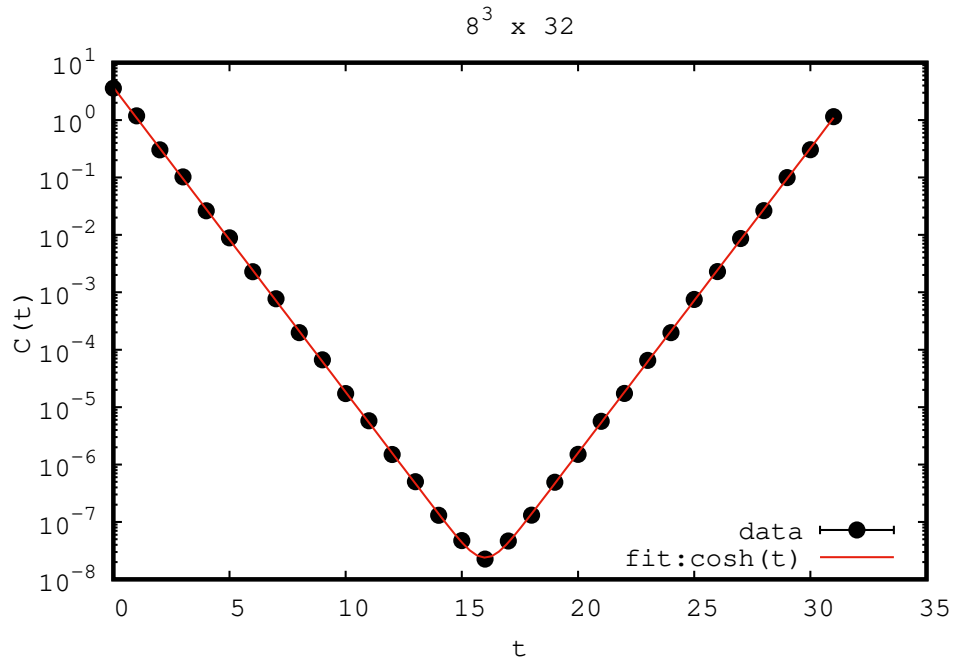


Figure 5.8:  $\langle C(t) \rangle$ : pion correlator with quark mass  $m = 0.2$  for  $8^3 \times 32$

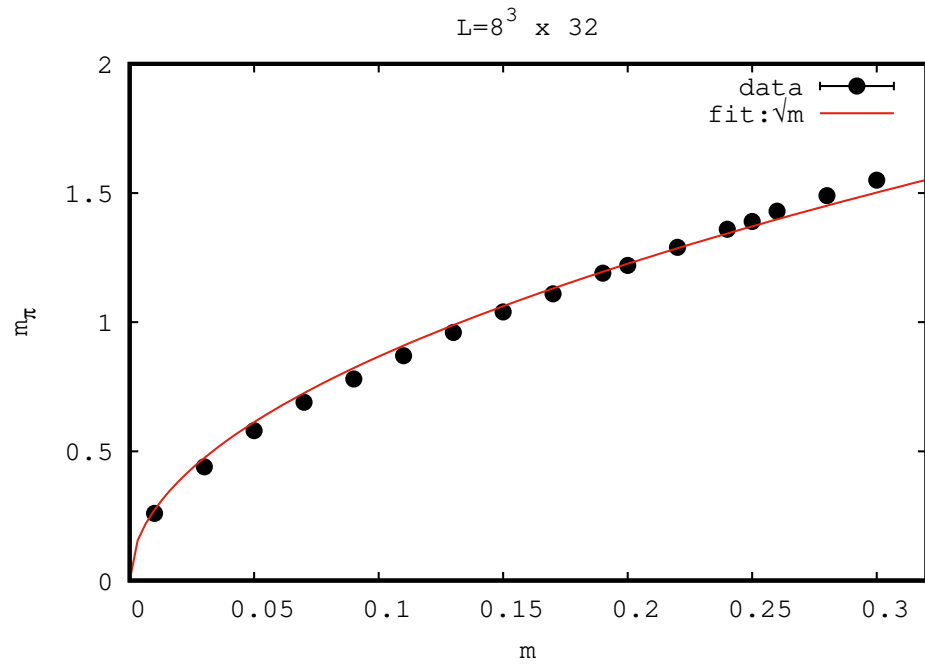


Figure 5.9:  $m_\pi$  vs  $m$ : Pion mass vs bare quark mass for  $8^3 \times 32$

## 5.4 Summary

We performed first studies of  $SU(2)$  lattice gauge theory with dynamical reduced staggered fermions. The pseudo-real nature of the fundamental representation of  $SU(2)$  allows us to employ the standard RHMC algorithm without encountering a sign problem. Unlike  $SU(N)$  for  $N > 2$  a gauge invariant site mass term is allowed and we investigate the model including both this term and a gauge invariant one-link mass operator. We find strong evidence that a site bilinear fermion condensate is formed at strong coupling spontaneously breaking an exact  $U(1)$  symmetry down to  $Z_2$ . We find good evidence for the corresponding Goldstone boson - the pion. These results are consistent with previous studies that used the spectrum of low-lying eigenmodes of the quenched Dirac operator to find evidence for chiral symmetry breaking in this theory. Our results strengthen these conclusions and support the analysis given in [35]. This work is motivated by an attempt to understand some of the novel phase structure in a related Higgs-Yukawa model involving reduced staggered fermions interacting with  $SU(2)$  gauge fields. Current work establishes the bedrock for understanding the results of related Higgs-Yukawa model in a gauge-theoretic setup. In gauged model fermion bilinear condensation through spontaneous symmetry breaking is strictly prohibited by enhancing the protecting symmetry from global to gauge symmetry.

# Chapter 6

## Four-fermion condensates in $SU(2)$ Yang-Mills-Higgs theory on lattice

### 6.1 Introduction

In expanded phase diagram discussed in chapter 3 there is evidence for a direct transition between massless and massive phase is possible. Since there is no symmetry breaking this novel transition eludes a Landau-Ginzburg description in terms of a local order parameter. Instead the transition is argued to result from a proliferation of topological defects in the scalar field [10].

This phenomenon of symmetric mass generation has also received a great deal of interest in condensed matter physics [5, 12] and in three dimensions this phenomenon was conjectured to be described by a gauge theory [23].

The Higgs-Yukawa models that have been used to generate this novel structure are invariant under an  $SO(4)$  symmetry and utilize a scalar field which transforms in the adjoint representation of one of the  $SU(2)$  factors making up  $SO(4) = SU(2) \times SU(2)$ . In the rest of this paper we call this  $SU_+(2)$ . This scalar is a singlet under the other factor which we call  $SU_-(2)$ . It is then rather

natural to imagine replacing the adjoint scalar field with a corresponding gauge field and ask whether the resulting gauge theory is capable of generating a four fermion condensate even in the absence of a Yukawa coupling. In practice we have considered a model containing both scalars and gauge fields and tried to map out the resulting phase diagram.

We expect for small Yukawa coupling that the theory is in a confined phase while for weak gauge coupling and large Yukawa coupling one might expect to see the four fermion condensate which can be interpreted as a Higgs phase of the theory. It is plausible that one might expect to see a line of phase transitions separating these two phases in the two dimensional phase diagram spanned by the Yukawa and gauge couplings.

## 6.2 Fermion kinetic term

Consider staggered fermions in the bifundamental representation of an  $SU(2) \times SU(2)$  symmetry. The fermions transform under a general gauge transformation as

$$\psi \rightarrow G\psi H^\dagger \quad (6.1)$$

where  $G \in SU_+(2)$  and  $H \in SU_-(2)$ . The above transformation with left and right action of the group is equivalent to the standard tensor transformation

$$\psi^{Aa} = G^{AB} H^{*ab} \psi^{Bb} \quad (6.2)$$

To construct the model we start with the full staggered action given in (6.3) gauged under both  $SU(2)$  factors:

$$S_F = \sum_{x,\mu} \frac{1}{2} \eta_\mu(x) \text{Tr} [\psi^\dagger(x) U_\mu(x) \psi(x+\mu) V_\mu^\dagger(x) - \psi^\dagger(x) U_\mu^\dagger(x-\mu) \psi(x-\mu) V_\mu(x-\mu)] \quad (6.3)$$

This action is invariant under the following gauge transformations

$$\begin{aligned}
\psi(x) &\rightarrow G(x)\psi(x)H^\dagger(x) \\
U_\mu(x) &\rightarrow G(x)U_\mu(x)G^\dagger(x+\mu) \\
V_\mu(x) &\rightarrow H(x+\mu)V_\mu(x)H^\dagger(x)
\end{aligned}
\tag{6.4}$$

The only single site gauge invariant mass term for fields in the bifundamental representation is  $Tr(\psi^\dagger\psi)$  which vanishes on account of the Grassmann nature of the fields. We can, however, construct a gauge invariant four-fermion term given in (6.5)

$$Tr(\psi^\dagger\psi\psi^\dagger\psi) \tag{6.5}$$

which is non-zero and yields the usual four fermion term.

### 6.3 Imposing the reality condition

The equivalence between this model and the original four fermi models requires the imposition of two further constraints. First we need to impose a reality condition on the fermions to reduce to four real degrees of freedom and second we will eventually set the gauge coupling for  $SU_-(2)$  to zero and set  $V_\mu(x) = I$ . For the moment let us focus the first of these which is equivalent to imposing the constraint

$$\psi^\dagger = \sigma_2\psi^T\sigma_2 \tag{6.6}$$

This implies that the fermion field can be written in terms of four real components  $\chi_\mu, \mu = 1 \dots 4$

$$\psi = \sum_\mu \chi_\mu\sigma_\mu \tag{6.7}$$



where  $\sigma_\mu = (I, i\sigma_i)$  and the original  $SO(4)$  fields can be recovered using the relation

$$\chi_\mu = \frac{1}{2}Tr(\sigma_\mu\psi) \quad (6.8)$$

Notice that the previous four fermion term  $Tr(\psi^\dagger\psi\psi^\dagger\psi)$  reduces to the simple form  $\chi_1\chi_2\chi_3\chi_4$  after this. Making use of this condition we can write the action as

$$S_F = \sum_{x,\mu} \frac{1}{2}\eta_\mu(x)Tr[\psi^T(x)\mathcal{U}_\mu(x)\psi(x+\mu)\mathcal{V}_\mu^T(x) - \psi^T(x)\mathcal{U}_\mu^T(x-\mu)\psi(x-\mu)\mathcal{V}_\mu(x-\mu)] \quad (6.9)$$

where

$$\begin{aligned} \mathcal{U}_\mu(x) &= \sigma_2 U_\mu(x) \\ \mathcal{V}_\mu(x) &= -V_\mu(x)\sigma_2 \end{aligned} \quad (6.10)$$

This fermion operator is manifestly anti-symmetric

$$M = \sum_\mu \mathcal{U}_\mu(x)\delta(x+\mu, x)\mathcal{V}_\mu^T(x) - \mathcal{U}_\mu^T(x-\mu)\delta(x-\mu, x)\mathcal{V}_\mu(x-\mu) \quad (6.11)$$

where  $\mathcal{V}$  acts from the right. This form of the action leads to a Pfaffian rather than a determinant after the fermion integration. Moreover this fermion operator inherits the reality condition

$$M^* = \sigma_2 M \sigma_2 \quad (6.12)$$

Combining anti-symmetry and pseudo-reality we expect  $M$  to exhibit a quartet of complex eigenvalues  $(\lambda, \bar{\lambda}, -\lambda, -\bar{\lambda})$ . This guarantees that the fermion operator will have generically possess a real, positive definite Pfaffian. The exception to this will be if the operator develops a purely real eigenvalue. We have not observed this to be the case in our work.

In fact the situation is even better than this. Let us now return to the second constraint on the model. The model we are finally interested has only one set of gauge fields corresponding to  $SU_+(2)$ . If the gauge links corresponding to  $SU_-(2)$  ( $V_\mu(x) = \infty$ ) are set to unity all the eigenvalues of  $M$  are doubled and positivity is then completely guaranteed.

## 6.4 Adding Yukawa interactions

To facilitate the formation of a gauge invariant four fermion interaction we add the term given in (6.5) after which the action is

$$S_F = \frac{1}{2} \sum_{x,\mu} \eta_\mu(x) Tr[\psi^T(x) \mathcal{U}_\mu(x) \psi(x+\mu) \sigma_2] - \frac{1}{2} \sum_{x,\mu} \eta_\mu(x) Tr[\psi^T(x) \mathcal{U}_\mu^T(x-\mu) \psi(x-\mu) \sigma_2] + \frac{G^2}{4} \sum_x Tr(\psi^T \sigma_2 \psi \sigma_2 \psi^T \sigma_2 \psi \sigma_2) \quad (6.13)$$

As usual an action quadratic in fermionic variables can be achieved if we introduce an auxiliary field. In this case there are two fermion bilinears defined in (6.14) each of which transforms in the adjoint representation under one of the  $SU(2)$ 's and is a singlet under the other. Here we have used  $\psi^\dagger$  rather than  $\psi^T$  to exhibit more clearly the transformation properties of each bilinear.

$$\begin{aligned} \psi^\dagger \psi &\rightarrow H \psi^\dagger \psi H^\dagger \\ \psi \psi^\dagger &\rightarrow G \psi \psi^\dagger G^\dagger \end{aligned} \quad (6.14)$$

The two possible auxiliary fields  $\phi(x)$  and  $\sigma(x)$  must transform as

$$\begin{aligned} H \sigma H^\dagger \\ G \phi G^\dagger \end{aligned} \quad (6.15)$$

Since in the end we will choose to gauge only  $SU_+(2)$  we choose to include only the  $\phi$  auxiliary field in our work.

$$\begin{aligned}
S_F &= \frac{1}{2} \sum_{x,\mu} \eta_\mu(x) \text{Tr}[\psi^T(x) \mathcal{U}_\mu(x) \psi(x+\mu) \sigma_2] \\
&\quad - \frac{1}{2} \sum_{x,\mu} \eta_\mu(x) \text{Tr}[\psi^T(x) \mathcal{U}_\mu^T(x-\mu) \psi(x-\mu) \sigma_2] \\
&\quad + \frac{G}{2} \sum_x \text{Tr}[\psi^T(x) \sigma_2 \phi(x) \psi(x) \sigma_2] + \frac{1}{2} \sum_x \text{Tr}[\phi^2]
\end{aligned} \tag{6.16}$$

Notice that the field  $\phi$  is strictly forbidden from picking up a vev as that would imply spontaneous breaking of gauge symmetry which is forbidden in a lattice gauge theory<sup>1</sup>. To test for spontaneous breaking of the global  $SU_-(2)$  symmetry we can also add a gauge invariant mass term given in (6.17) to the action

$$m \sum_x \text{Tr}[\sigma_3 \psi^\dagger \psi] \tag{6.17}$$

This term explicitly breaks  $SU_-(2) \rightarrow U(1)$ . Finally, for the gauge part of action we have employed the standard Wilson action

$$S_G = \sum_x \sum_{\mu < \nu} -\frac{\beta}{2N} \text{Tr}[U_{\mu\nu}(x) + U_{\mu\nu}^\dagger(x)] \tag{6.18}$$

## 6.5 Reduction to $SO(4)$ model

To connect this model to the original  $SO(4)$  model studied in [3] we consider the limit  $\beta \rightarrow \infty$  which allows us to set  $U_\mu(x) = \mathbb{1}$ . The fermion operator then

---

<sup>1</sup>Unfortunately while  $\phi$  is a singlet Under  $SU_-(2)$  it does not obey the reality condition so that octet structure of eigenvalues of the fermion operator is reduced once again to quartets.

reduces to a symmetric difference operator and the action becomes

$$S = \sum_{x,\mu} \frac{1}{2} Tr[\psi^T \sigma_2(\eta \cdot \Delta) \psi \sigma_2] + \frac{G}{2} \sum_x Tr[\psi^T(x) \sigma_2 \phi(x) \psi(x) \sigma_2] + \frac{1}{2} \sum_x Tr[\phi^2(x)] \quad (6.19)$$

Transforming in the fundamental of  $SO(4)$  one finds

$$S = \sum_{x,\mu} \frac{1}{2} \chi^a(\eta \cdot \Delta) \delta^{ab} \chi^b + \frac{G}{2} \sum_x [\phi_1(\chi_1 \chi_2 + \chi_3 \chi_4) + \phi_2(\chi_1 \chi_3 + \chi_2 \chi_4) + \phi_3(\chi_1 \chi_4 + \chi_2 \chi_3)] + \frac{1}{2} \sum_x (\phi_i)^2 \quad (6.20)$$

Notice that the fermion bilinears appear in the self-dual representation of  $SO(4)$  in these variables. This projection on self-dual fields can then be transferred to the auxiliary field and after performing the trace over  $SU(2)$  indices we recover the  $SO(4)$  invariant action studied in [3]

$$S = \sum_{x,\mu} \frac{1}{2} \chi^a [(\eta \cdot \Delta) \delta^{ab} + \frac{G}{2} \phi_+^{ab}] \chi^b + \frac{1}{2} \sum_x (\phi_+^{ab})^2 \quad (6.21)$$

## 6.6 Numerical Results

Now we come to some preliminary results obtained by using the RHMC algorithm to simulate the model in (6.16). Our code utilizes the MILC libraries to allow for efficient parallelization to allow for studies on large lattice. However, our results so far have been confined to a small volume  $4^4$  lattice suitable for testing and validation of the code.

One important test of our code is whether we recover the known behavior of the  $SO(4)$  model in the weak gauge coupling limit. For this purpose we switch off the gauge fields and scan the four fermion condensate as a function of  $G$ . This is plotted in Fig. 6.1(left). Another proxy observable for the four fermion (massive) phase is  $Tr(\phi^2)$  which is plotted in Fig. 6.1(right). This plots are consistent with

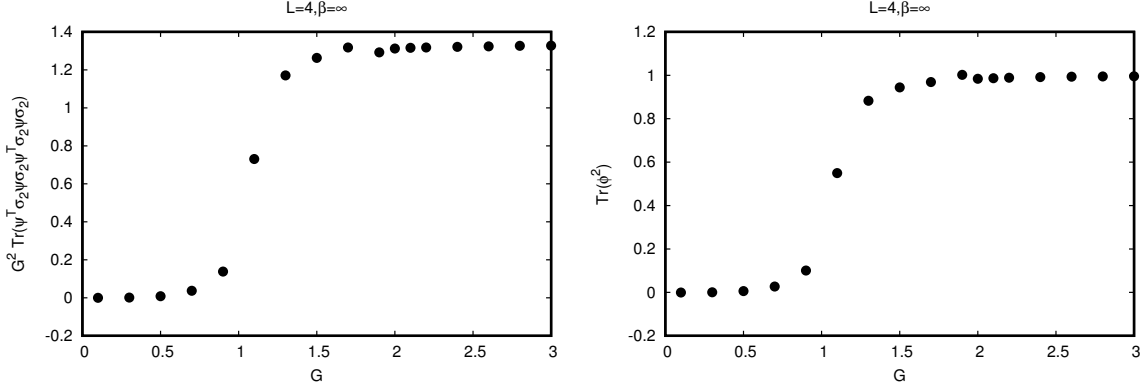


Figure 6.1: Four-fermion condensate(left) and  $\text{Tr}(\phi^2)$  (right) vs  $G$  with  $\beta = \infty$  for  $L = 4$

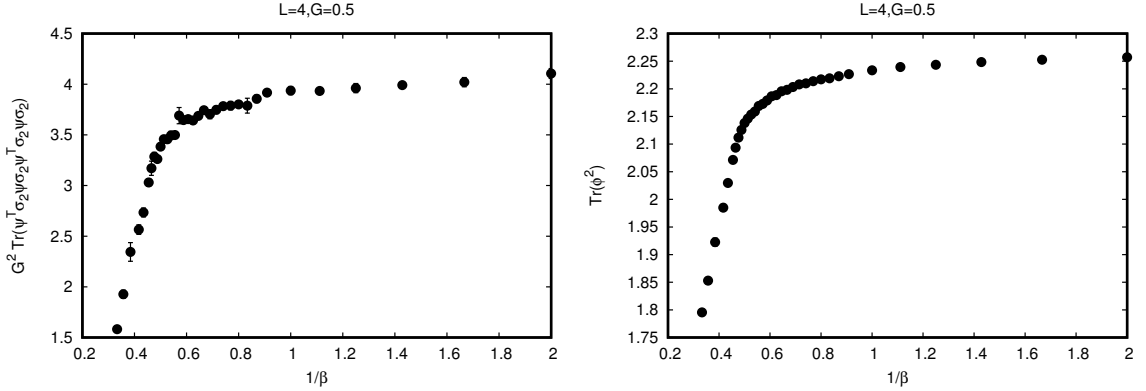


Figure 6.2: Four-fermion condensate(left) and  $\text{Tr}(\phi^2)$  (right) vs  $1/\beta$  with  $G = 0.5$  for  $L = 4$

those reported in [3]. Of course our main goal is to try to realize a four fermion phase through gauge interactions. As a first step in this direction we plot in Fig. 6.2 the four fermion condensate and  $\langle \text{Tr}(\phi^2) \rangle$  vs  $1/\beta$  at  $G = 0.5$ . At strong gauge coupling the four fermion condensate rises rapidly to a non-zero constant value. Notice that this value of  $G$  would not be sufficient to realize a four fermion phase in the absence of gauge interactions. It remains to map out this transition line for a range of  $G$  (using much larger lattice volumes).

## 6.7 Summary

In this chapter we have embedded an  $SO(4)$  invariant four-fermion model into a gauge model by gauging one of the two  $SU(2)$  subgroups of  $SO(4)$ . We have described in some detail the construction of the model in terms of a staggered fermion field transforming in the bi-fundamental representation of  $SU(2) \times SU(2)$  and how this representation can be related to the original fundamental representation of  $SO(4)$  by imposing a suitable reality condition on the fermions. Our numerical work is only just beginning but confirms that the model does indeed reduce to the original four fermion model in the limit the gauge coupling is sent to zero. Once the gauge coupling is turned on we have so far only run with a single value of the Yukawa coupling on a small lattice but our results are compatible with the appearance of a four fermion phase driven in part by strong gauge interactions. We interpret the four fermion phase as the (gauge invariant) signal of a Higgs phase in the gauge theory. Future work will aim to map out the phase diagram of the model using much larger lattices and understand the nature of any critical lines encountered. It will be particularly interesting to see whether the four fermion phase survives the limit in which the Yukawa coupling is sent to zero.

# Bibliography

- [1] V. Ayyar and S. Chandrasekharan, Phys. Rev. **D91**, 065035 (2015), [1410.6474](#).
- [2] V. Ayyar and S. Chandrasekharan, Phys. Rev. **D93**, 081701 (2016), [1511.09071](#).
- [3] S. Catterall and D. Schaich, Phys. Rev. **D96**, 034506 (2017), [1609.08541](#).
- [4] S. Catterall, JHEP **01**, 121 (2016), [1510.04153](#).
- [5] Y.-Y. He, H.-Q. Wu, Y.-Z. You, C. Xu, Z. Y. Meng, and Z.-Y. Lu, Phys. Rev. **B94**, 241111 (2016), [1603.08376](#).
- [6] V. Ayyar and S. Chandrasekharan, JHEP **10**, 058 (2016), [1606.06312](#).
- [7] V. Ayyar, PoS **LATTICE2016**, 327 (2016), [1611.00280](#).
- [8] D. Schaich and S. Catterall, EPJ Web Conf. **175**, 03004 (2018), [1710.08137](#).
- [9] W. Bock, J. Smit, and J. C. Vink, Phys. Lett. **B291**, 297 (1992), [hep-lat/9206008](#).
- [10] S. Catterall and N. Butt, Phys. Rev. **D97**, 094502 (2018), [1708.06715](#).
- [11] L. Fidkowski and A. Kitaev, Phys. Rev. **B81**, 134509 (2010), [0904.2197](#).

- [12] T. Morimoto, A. Furusaki, and C. Mudry, Phys. Rev. **B92**, 125104 (2015), [1505.06341](#).
- [13] D. Stephenson and A. Thornton, Phys. Lett. **B212**, 479 (1988).
- [14] A. Hasenfratz and T. Neuhaus, Phys. Lett. **B220**, 435 (1989).
- [15] I.-H. Lee, J. Shigemitsu, and R. E. Shrock, Nucl. Phys. **B330**, 225 (1990).
- [16] I.-H. Lee, J. Shigemitsu, and R. E. Shrock, Nucl. Phys. **B334**, 265 (1990).
- [17] W. Bock and A. K. De, Phys. Lett. **B245**, 207 (1990).
- [18] A. Abada and R. E. Shrock, Phys. Rev. **D43**, 304 (1991).
- [19] A. Hasenfratz, P. Hasenfratz, K. Jansen, J. Kuti, and Y. Shen, Nucl. Phys. **B365**, 79 (1991).
- [20] P. Gerhold and K. Jansen, JHEP **0709**, 041 (2007), [0705.2539](#).
- [21] P. Gerhold and K. Jansen, JHEP **0710**, 001 (2007), [0707.3849](#).
- [22] M. F. L. Golterman, D. N. Petcher, and E. Rivas, Nucl. Phys. **B395**, 596 (1993), [hep-lat/9206010](#).
- [23] Y.-Z. You, Y.-C. He, C. Xu, and A. Vishwanath, Phys. Rev. **X8**, 011026 (2018), [1705.09313](#).
- [24] T. Banks, Y. Dothan, and D. Horn, Phys. Lett. **117B**, 413 (1982).
- [25] M. F. L. Golterman and J. Smit, Nucl. Phys. **B245**, 61 (1984).
- [26] C. van den Doel and J. Smit, Nucl. Phys. **B228**, 122 (1983).
- [27] P. van Baal and A. Wipf, Phys. Lett. **B515**, 181 (2001), [hep-th/0105141](#).
- [28] Y. He and H. Guo, Phys. Lett. **B739**, 83 (2014), [1405.4089](#).



- [29] Y. BenTov and A. Zee, Phys. Rev. **D93**, 065036 (2016), [1505.04312](#).
- [30] E. Eichten and J. Preskill, Nucl. Phys. **B268**, 179 (1986).
- [31] Y.-Z. You and C. Xu, Phys. Rev. **B91**, 125147 (2015), [1412.4784](#).
- [32] S. Aoki et al., Eur. Phys. J. **C77**, 112 (2017), [1607.00299](#).
- [33] E. Follana, C. T. H. Davies, and A. Hart (HPQCD, UKQCD), PoS **LAT2006**, 051 (2006).
- [34] S. Catterall and A. Veernala, Phys. Rev. **D87**, 114507 (2013), [1303.6187](#).
- [35] P. H. Damgaard, U. M. Heller, R. Niclasen, and B. Svetitsky, Nucl. Phys. **B633**, 97 (2002), [hep-lat/0110028](#).
- [36] S. Catterall and N. Butt (2018).
- [37] M. A. Clark and A. D. Kennedy, Nucl. Phys. Proc. Suppl. **129**, 850 (2004), [850(2003)], [hep-lat/0309084](#).

Curriculum Vitae  
**Nouman Tariq Butt**

Department of Physics, Syracuse University,  
Physics Building, Room: 312, Syracuse, NY 13244

*Phone:* (315) 876-6370

*Email:* ntbutt@syr.edu

---

**Education**

---

- **Phd Physics** *December 2019*  
Senior graduate GPA: 3.58/4  
Department of Physics  
Syracuse University  
Research: Strongly coupled fermions on the lattice  
Advisor: Prof. Simon Catterall
- **BS Physics** *Oct 2008 - May 2012*  
Lahore University of Management Sciences, Pakistan

---

**Employment**

---

- **QIS Postdoctoral Researcher** *Jan 2020 - Jan 2021*  
Argonne National Lab

---

## Publications and Pre-prints

---

- Topology and strong four fermion interactions in four dimensions [Phys. Rev. D 97, 094502](#)
- Simulations of  $SU(2)$  lattice gauge theory with dynamical reduced staggered fermions [Phys Rev D 99 014505](#)
- $SO(4)$  invariant Higgs-Yukawa model with reduced staggered fermions [Phys.Rev. D.98.114514](#)
- Four fermion condensates in  $SU(2)$  Yang-Mills-Higgs theory on a lattice [arXiv:1811.01015](#)  
(submitted to Proceedings of 36th Annual International Symposium on Lattice Field Theory - LATTICE2018 22-28 July, 2018)
- Tensor network formulation of the massless Schwinger Model [arXiv:1911.01285](#)
- Tensor network computation using Quantum Circuits...*In progress*

---

## Teaching Experience

---

- \* Grader for Phy 661(Quantum Mechanics) and Phy 581 (Methods of Theoretical Physics) Fall 2014



---

\* **Invited Talk:** Phase diagram of strongly interacting four-fermion theory (April 7 2018) at [LBSM 2018, UC Boulder](#)

\* **Contributed Talk:**  
Phase diagram of strongly interacting Higgs-Yukawa theory (July 23 2018) at [Lattice 2018, Michigan State University](#)

\* **Poster:**  
Symmetric mass generation through non-abelian gauge fields (July 25 2018) at [Lattice 2018, Michigan State University](#)

---

## Technical Skills

---

**Programming Languages:** C/C++, Bash, Python, QISKIT

**High-Performance Computing:** MILC , TensorFlow, TensorNetwork API

**System Administration:** Macintosh, GNU/Linux , Windows

**Markup:** Mathematica,  $\text{\LaTeX}$

---

## Conferences

---

\* Lattice BSM April 2017 - Boston University

\* Lattice BSM April 2018 - UC Boulder

\* Lattice 2018 July 2018 - Michigan State University

---

## Professional References

---

\* Simon Catterall

Professor of Physics and Department Associate Chair

Syracuse University, Syracuse NY USA

Email: smcatterall@gmail.com

\* David Schaich

Lecturer in Theoretical Physics

University of Liverpool, Liverpool UK

Email: daschaich@gmail.com

\* Yannick Meurice

Professor of Physics

University of Iowa , Iowa City, Iowa 52242

Email: yannick-meurice@uiowa.edu

\* James Osborn

Computational Scientist / Catalyst Team Lead

Argonne National Laboratory , Lemont IL USA

Email: osborn@alcf.anl.gov

---